Aquaculture
March 2019, Volume 503, Pages 231-241
https://doi.org/10.1016/j.aquaculture.2018.12.082
https://archimer.ifremer.fr/doc/00474/58559/

Changes in planktonic microbial components in interaction with juvenile oysters during a mortality episode in the Thau lagoon (France)

Richard Marion [1, *], Bec Beatrice [2], Vanhuysse Charles [1, 2], Mas Sébastien [3], Parin David [3], Chantalat Camila [1], Le Gall Patrik [1], Fiandrino Annie [1], Lagarde Franck [1], Mortreux Serge [1], Ouisse Vincent [1], Rolland Jean-Luc [4], Degut Anaïs [1], Hatey Elise [2], Fortune Martine [1], Roque D'Orbcastel Emmanuelle [1], Messiaen Gregory [1], Munaron Dominique [1], Callier Myriam [5], Oheix Jocelyne [1], Derolez Valerie [1], Mostajir Behzad [2]

[1] MARBEC UMR UM, CNRS, Ifremer, IRD, Sète, France
[2] MARBEC UMR UM, CNRS, Ifremer, IRD, Montpellier, France
[3] MEDIMEER UMS, SMEL, 2 rue des Chantiers, Sète, France
[4] IHPE UMR 5244 Univ. Perpignan Via Domitia, CNRS, UM, Place Eugène Bataillon, 34095 Montpellier, France
[5] MARBEC UMR UM, CNRS, Ifremer, IRD, Palavas, les Flots, France

* Corresponding author : Marion Richard, email address : marion.richard@ifremer.fr

Abstract :

Oysters modify the planktonic microbial community structure by their filtration and NH_4 excretion activities. While many studies have been conducted on this subject with adult oysters, none had been carried out in situ with juveniles. Pacific oyster juveniles (*Magallana gigas,* previously *Crassostrea gigas*) died massively all over the world since 2008 in relation with OsHV-1 infection. During mortality episodes, sick and dead oysters are not separated from healthy live ones, and left to decay in the surrounding environment, with unknown consequences for the nutrient cycle and planktonic microbial components (PMC). The present study aimed to elucidate for the first time the interactions between oyster juveniles and PMC during a mortality episode. Innovative 425-L pelagic chambers were deployed weekly in situ around oyster lanterns along a stocking-density gradient in the Thau Mediterranean lagoon (France) before, during and after an oyster mortality episode, from April to May 2015. This study reveals (i) significant changes of planktonic microbial community structure during mortality episodes, with a proliferation of picoplankton (<3 µm) and ciliates (*Balanion* sp.*, Uronema* sp.) within 2 weeks when mortality rates and numbers of moribund juvenile oysters were highest. These changes were probably induced by oyster tissue leaching, decomposition and mineralization, which probably began during the moribund period, as suggested by an increase of PO_4 concentration and N:P ratio decrease, (ii) oyster juveniles mainly retained 3–20 µm plankton. In contrast to adults, picophytoplankton and small heterotrophic flagellates (<3 µm) were significantly depleted in the presence of oyster juveniles. Depletion of picoplankton occurred only at the starting of the mortality episode and during the moribund phase. (iii) Oyster juvenile filtration and mortality shifted the planktonic microbial structure toward a heterotrophic microbial system, where ciliates and heterotrophic flagellates acted as a trophic link between picoplankton and oysters. The next stage of our investigation is to examine the effect of a mortality episode on pathogen fluxes in the water column, exploring their relationships with planktonic

components and dead oyster flesh.

Highlights

► The planktonic microbial components (PMC) change during OsHV-1 oyster juvenile mortality. ► Picophytoplankton and ciliates increase during infection and mortality periods. ► Filtration and mortality of juvenile oysters shift PMC toward a heterotrophic system.

Keywords : *Magallana gigas*, *Crassostrea gigas*, Spat, OsHV-1 µVar, Mortality, Picoplankton, Heterotrophic flagellates, Ciliates, *Uronema*, *Balanion*

1. Introduction

Shellfish farms are known to modify particulate fluxes through bivalve activities: i.e. (i) filtration (Dupuy et al. 2000, Trottet et al. 2008), (ii) excretion (Mazouni 2004, Richard et al. 2006, 2007, Jansen et al. 2011), and (iii) biodeposition (Callier et al. 2006, 2009, Robert et al. 2013). At high stocking densities in confined environments, shellfish such as mussels and oysters can affect the seston biomass load via filtration (Smaal et al. 2013, Filgueira et al. 2014a, b), stimulate primary production via nitrogen excretion (Chapelle et al. 2000, Souchu et al. 2001, Mazouni 2004) and modify the microbial plankton community structure (Dupuy et al. 1999, 2000, Froján et al. 2014, Mostajir et al. 2015). During filtration processes, oysters can remove particles from the water column using pallial organs (gills, labial palps and mantle). Particles in suspension are 1) either selectively retained by gills, transported to the mouth to be ingested, digested and excreted as feces forms by anus in the exhalant cavity; or 2) forward to the labial palps to be rejected in the inhalant cavity as pseudofeces depending on qualitative and/or size selection (Gosling 2015, Bayne 2017). At the adult stage, oysters trap particles ranging from 3-5 µm (Barillé et al. 1993, Dupuy et al. 1999, 2000) to 500 µm (Barillé et al. 1993, Tamburri & Zimmer-Faust 1996, Lam-Hoai et al. 1997, Dupuy et al. 2000, Troost et al. 2008), including nano- (3–20 µm) and microplankton (20–200 µm), comprising of phyto-, protozoo- and metazoo plankton. Examining the microbial Autotroph: Heterotroph C biomass ratio (A:H) structural index, oyster activities make the microbial food web more heterotrophic in a confined environment (Mostajir et al. 2015).

The production cycle of oysters includes two stages in a subtidal environment: a pre-growing phase during which oyster juveniles are reared in suspended lanterns and a second phase during which they are reared on ropes. Since 2008, juvenile oysters have been decimated by OsHV-1 µVar virus infections at levels ranging from 40 to 100% in French oyster farming areas (Garcia et al. 2011, Pernet et al. 2012). Currently, OsHV-1 is observed

throughout the world (Mineur et al. 2014). Although many studies have explored the consequences of this infection for oysters (Tamayo et al. 2014, Corporeau et al. 2014, Green et al. 2016), only one has investigated the consequences of these mortality events in the environment (Richard et al. 2017). Unlike most other animal production industries, sick and dead individuals are not separated from conspecifics in shellfish farms, which can favour cross-contamination and disease spreading. Dead oysters are kept in the rearing environment until their flesh totally disappears. Using a laboratory approach, Richard et al. (2017) showed that mortality of oyster juveniles leads to a significant increase of ammonium and phosphate fluxes and a decrease in the N:P ratio in relation to the decomposition and mineralization of oyster flesh with a possible impact on the planktonic community structure.

Although the pre-growing stage is a key stage in the oyster production cycle, and mortality is a crucial topic, no *in situ* studies have yet described the influence of juvenile oysters and mortality events on planktonic components. This topic remains unknown.

We firstly hypothesised that under normal conditions, the influence of juveniles on the planktonic microbial components would be different from that of adults considering that optimum spectrum retention and metabolism of bivalves would depend on their size (Gosling 2015). Secondly, we put forward the hypothesis that during mortality events, decomposition of oyster flesh may lead to ammonium and phosphate increases and a decrease in the N:P ratio in the environment as observed in experimental laboratory conditions (Richard et al. 2017), which may induce changes in microbial planktonic components. Indeed, ammonia release at the interface of dead organisms may stimulate primary production and specifically favour blooms of small-sized phytoplankton, i.e., picophytoplankton, as observed via the NH_4 excretion of adult oysters (Chapelle et al. 2000, Souchu et al. 2001). High PO_4 inputs related to oyster decomposition may increase the abundance of prokaryotes, picoeukaryotes and cyanobacteria, as it has been observed during a P-enrichment experiment in microcosms

(Tsiola et al. 2015). In parallel, we put forward the hypothesis that proliferation of heterotrophic organisms such as prokaryotes and ciliates could be induced by the presence of decaying oyster flesh in the water column, as already observed in hatcheries during mortality events (Plunket & Hidu 1978, Elston et al. 1999). Finally, we hypothesised that the system's trophic status may shift toward heterotrophy via both filtration of oyster juveniles as observed for oysters at the adult stage (Mostajir et al.2015), and decomposition of oyster flesh.

The objective of this study, which is part of the MORTAFLUX program, was to test these hypotheses using an *in situ* approach in order, (i) to describe the temporal dynamics of planktonic microbial components (PMC) and (ii) to examine the interactions of juvenile oysters with PMC and the trophic status of the Thau lagoon system during a mortality episode. Our approach involved the use of innovative 425-L pelagic chambers, along a stocking-density gradient, before, during and after a mortality event. The pelagic chambers were used to estimate temporal planktonic microbial component variations in an enclosed system in the presence and absence of oysters to highlight oyster juvenile interactions with planktonic microbial components. Differences between final and initial plankton concentrations recorded in the presence of oysters, corrected by observed processes in the absence of oysters (planktonic production, predation or mortality), and related to pelagic chamber volume and incubation time enabled the determination of negative fluxes that were interpreted as quantity of depleted plankton per hour and per lantern via oyster filtration, without details being given on ingestion or rejection pathways. The data gathered were used to help describe changes of PMC and interactions with oyster juveniles during a mortality event in order to better understand the consequences of this phenomenon on planktonic microbial components.

1. Materials and methods

1.1. Experimental design and devices

The experiment was carried out from March to June 2015 in Thau Lagoon, on the French Mediterranean coast (43°22'44.87''N, 3°34'37.64'E). At the end of March 2015, 27 000 juvenile oysters were sent to Sète by SCEA Charente Naissains. These juveniles originated from the Marennes-Oléron basin (45°58'16.08''N, 01°06'16.2''W) where they were collected by SCEA on spat collectors in July 2014 and where they have grown until their harvesting and shipment to Sète for the experiment. The mean total wet weight (WW) and length (± SD) measured on arrival at the Laboratory in Sète were 0.49 ± 0.02 WWg and 1.8 ± 0.02 cm, respectively. After two days of acclimation in laboratory tanks, the juveniles were put into eighteen suspended lanterns composed of seven storeys at 100, 200, 350 individuals per storey (i.e., 0, 700, 1400 or 2450 oysters.lantern^{-1}, Fig. 1A). The lanterns were then suspended from an experimental table and immersed in Thau Lagoon. Two empty lanterns (0 oyster.lantern^{-1}) were used as a control (0). Before, during and after the mortality event, 425-L pelagic chambers (150 cm Height, 60 cm Ø, Fig. 1B) were deployed weekly by scuba divers around two sets of 4 lanterns that either contained no oysters (0) or contained low, medium and high densities of oysters (4 levels of Density: 0, 100, 200, 350 ind.storey^{-1}). The maximum density (350 ind. storey^{-1}) was used by our shellfish farmer partner. The lanterns were separated by more than two meters to allow divers to swim easily with pelagic chamber around the lanterns without hitting the lanterns and causing resuspension of feces or decaying flesh. Pelagic chambers were deployed around the lanterns for five hours during which pelagic chambers were closed. There was therefore no influence between different lanterns (ie. among different density levels) during incubation time. Incubation duration was limited to five hours to permit to measurement of significant dissolved and particulate fluxes without causing physiological stress to the juvenile oysters by oxygen depletion. Oxygen depletion did not exceed 20% and oxygen level always remained above 70% according to recorded values

by each of HOBO U26 Dissolved Oxygen loggers (Fig. 1). Water was sampled from each pelagic chamber at the beginning and end of the incubation (T0, Tf; Fig. 1) for each stocking density and sampling week. A number was allocated to each sampling week (W16 to W22) in relation to the 2015 annual calendar. Thus, W16 corresponded to the 13-19th April, W17 to 20-26 th April, W18 to 27 th April-3 th May, W19 to 4-10 th May, W20 to 11-17 th May, W21 to 18-24th May, and W22 to 25-31 th May 2015. In figures, the week number was preferred to date since the sampling of oysters and water was carried out during the same week but not during the same day.

1.2. Sampling and analyses

Juvenile oysters

Mortality and biometry

Throughout the experiments, the number of living, dead, and moribund oysters were counted weekly in the central storey of two lanterns per stocking density. Oysters were qualified as (i) dead, when their valves were open at emersion; (ii) alive, when their valves were closed at emersion; or (iii) moribund, when their valves were not well closed after pressure was exerted on the two valves and from which air bubbles escaped. At each sampling, dead oysters were excluded from the sampled storey. Instantaneous rates of mortality and moribund oysters were calculated from the number of dead or moribund individuals in the studied storey relative to the total number of oysters observed per week. Cumulative mortality rates were calculated each week from the sums of dead oyster numbers observed at each sampling relative to the initial number of oysters per storey. At the same time, each week, ten oysters were randomly sampled per storey for biometric analysis among the live and moribund oysters, and among dead organisms when possible depending on the

week. Shell lengths of live and dead oysters were determined with a calliper. Total and flesh weights of live and moribund oysters were determined with a precision balance to 10^{-3} g. Dry wet weights (DW) were measured after 48 hours of lyophilisation. Total weight of oysters and dry flesh per lantern (g DW lantern^{-1}) were calculated as follows: mean individual dry flesh weight × mean number of (live + moribund) oysters per storey × 7 storeys for each week and stocking density conditions. The effect of "storey location" (7 positions) was tested at the end of the experiment (June 2015) on mortality and the individual weight of oyster juveniles using six lanterns (3 density, 2 replicates). ANOVA showed no effect of storey location on mortality rate ($p = 0.22$) and individual weight ($p = 0.57$). Thus measurements carried out on the central storey are representative of the whole lantern.

OsHV-1 detection

Each week, two pools of three oysters were randomly sampled per central storey and per lantern. Oyster flesh were pooled in Eppendorf and stored in ethanol at -80°C for OsHV-1 analysis. Absolute quantification of OsHV-1 genome copies was estimated for each oyster sample as described in Richard et al. (2017). Genomic DNA was purified from pool of oyster tissues using the Wizard® SV Genomic DNA Purification System (Promega). OsHV-1 genomic DNA was detected and quantified using quantitative PCR (qPCR) (Pepin et al. 2008) with a Roche LightCycler 480 Real-Time thermocycler (qPHD-Montpellier GenomiX platform, Montpellier University). The PCR reaction volumes were 6 µL and contained LightCycler 480 SYBR Green I Master mix (Roche), 100 nM of pathogen-specific primers and 1µl of sample DNA. Pathogen-specific primer pairs C9/C10 were obtained from the literature (Barbosa-Solomieu et al. 2004, Schikorski et al. 2011) and their resulting amplification products were cloned into the pCR4-Topo vector. Plasmids were extracted using the Wizard Plus SV miniprep DNA purification system (Promega) and standard curves

of known concentration of plasmid were generated according to the Applied Biosystems manual of absolute real-time RT-PCR quantification. Absolute quantification of OsHV-1 genome copies in oyster samples was estimated by comparing the observed Cp values to known plasmid standards.

Histological assessment of oysters

During W19, fifteen moribund oysters were sampled from a lot of oyster juveniles which was deployed at the same experimental site and during the same period as the experimental oyster lanterns used in this study as part of the REPAMO (Réseau de Pathologie des Mollusques) network. Oysters were sent using cooler to the HISTALIM Laboratory for histological analysis. The HISTALIM lab is accredited for these analyses in accordance with the recognized international standard ISO/IEC 17025, issued by the French Committee for Accreditation (COFRAC Certificate n°1-1794 version 7). Procedures of sample conditioning and analyses were carried out according to the Manual of Diagnosis Tests for Aquatic Animals (OIE World Organisation for Animal Health 2018). At the lab, the oysters were opened by severing the adductor muscle. A cross section (3-5 mm) of each oyster including labial palps, gills, and digestive gland was fixed in Davison's solution. The section was dehydrated in an ethanol series and embedded in paraffin. The section was then stained with hematoxylin-eosin and observed under a light microscope for diagnosis. The images were exploited using the NanoZoomer Digital Pathology NPD software (Hamamatsu). Quantification of ciliates was carried out for each oyster sample.

Physico-chemical parameters and water sampling

In parallel to pelagic chamber deployment, temperature and salinity were measured using a WTW® probe at the beginning and at the end of incubation. Using a peristaltic pump, 5–10 L water samples were *in situ* carried out at the beginning and end of incubation for each pelagic chambers. Water samples were then transferred in coolers to the laboratory for analysis of chemical parameters and planktonic components.

Nutrients

At the laboratory, water samples were filtered through a 0.22-µm filter (Acetate Cellulose 47 mm) and stored at -20°C for analysis of ammonium, nitrate, nitrite and phosphate. Nutrient concentrations were measured using Seal AA3 analytical autoanalysers following previously described methods (Aminot and Kérouel 2007) with colorimetric detection (from SEAL Analytical, Germany) for PO_4, NO_3 and NO_2 and a fluorometric method (from JASCO, FP-2020plus, France) for NH_4. The Ifremer laboratory in Sète is accredited for these analyses, in accordance with the recognised international standard ISO/IEC 17025, issued by the French national accreditation body COFRAC (Certificate n°1-1655).

Planktonic Microbial Components

Autotrophic microorganisms

Autotrophic biomasses were analysed according to Bec et al. (2011). At the laboratory, 200 mL per sample were filtered through 3-µm (Nucleopore) and 20-µm (Nylon) membranes. The two 200 mL-samples of (<3, <20 µm) filtered water and a third sample of unfiltered water were then vacuum-filtered (<10 cm Hg) through a Whatman GF/F membrane (0.7 µm). Thus, a batch of three filters was available per sample. They retained fractions of > 0. 7 µm, > 3 µm

and > 20 µm. Thus, three filters per sample were stored at –20°C in glass tubes. The filters were then ground in acetone (90%) and extracted over 24 h in the dark at 4°C. Pigments were measured by spectrofluorimetry (Neveux & Lantoine 1993). Chlorophyll *a*, *b* and *c* (Chl*a*, Chl*b* and Chl*c*, respectively) concentrations (µg L^{-1} ± 5%) were calculated for each sample to determine pico- (0.7–3 µm), nano- (3–20 µm) and microphytoplankton (>20 µm) biomasses.

Heterotrophic micro-organisms

The following protocols were taken from (Mostajir et al. 2015) with some adaptations for this study. For the enumeration of heterotrophic prokaryotes, 1 mL of water per sample was fixed with 40 µl glutaraldehyde, frozen at −20°C, and kept at −80°C until analysis. Aliquots of thawed samples (300 µl) were stained with 8 µl SYBR Green I (Molecular Probes) for 15 min at 4°C in the dark (Marie et al. 1997). After adding 0.96- and 2-µm beads (PolySciences) and TruCount beads (with a known concentration, lot 49912, BD Biosciences) as an internal standard, the heterotrophic prokaryotes were enumerated and analyzed using a FACSCalibur (Becton-Dickinson) flow cytometer, fitted with a 488 nm, 15 mW, laser, for 2 to 3 min at a low rate (10–12 µl min^{-1}) using the FL1 detector (λ = 530 nm). All cytometric data were logged and analyzed using Cell Quest (Becton-Dickinson).

Heterotrophic flagellates (HF) were enumerated in three size classes: <3, 3−5, and 5−10 µm. The larger HF of >10 µm were not considered as they were observed only sporadically. 30 mL of water per sample were fixed with 0.2 µm pre-filtered formalin (4% final concentration) and kept at 4°C in the dark. Then 10 mL of sample were stained with 0.8 ml DAPI (4',6'-diamidino-2-phenyindole hydrochloride) and vacuum filtered (<7 kPa) through 25 mm black Nuclepore polycarbonate membrane (0.5 µm pore size). The filter was placed on a slide and examined using an epifluorescence microscope (Olympus AX 70) with a 100×

objective. By changing the excitation light of the epifluorescence microscope, heterotrophic organisms were distinguished from the autotrophic flagellate: HF were in blue colour while autotrophic flagellate appeared in pale pink colour. Ciliates were enumerated in five size classes (10−15, 15−20, 20−25, 25−30, and 30−40 µm) using an Olympus inverted microscope (IX-70) in 100 ml of water per sample that had been previously preserved with 2 mL commercial Lugol's solution and stored at 4°C in the dark. Enumeration and identification to the genus level was carried out after 24 h settlement in the dark (Utermöhl 1958). Larger ciliates (>40 µm) were not included in the counts because they were only sporadically present in the samples.

Given that counting of HF and the determination of ciliates require many hours of analysis, efforts were concentrated on (i) water samples describing the initial conditions without interaction with oysters (i.e., no oyster: [0], initial time: T0) and (ii) water samples taken at the final sampling time for the two contrasted oyster juvenile densities (100 and 350 ind. storey^{-1}: [100, 350]Tf) and during the most critical weeks (W17, W18 and W19). The selection of samples for analysis was made after a first analysis of mortality kinetics. As ciliates appeared to be an important component during the mortality episode, the initial dataset ([0]T0) was complete, in contrast to HF, whose abundances were only available for W17, W18 and W19.

1.3. Estimating carbon biomass for planktonic microbial components

The phytoplankton Chl*a* biomasses, heterotrophic prokaryote abundances and biovolumes of HF and ciliates were converted to equivalent carbon (C) biomass as in Mostajir et al. (2015). Chl*a* data were converted to C biomass using a value of 57 (Latasa et al. 2005), as carried out previously in a mesocosm experiment in the Thau lagoon (Vidussi et al. 2011).

Total heterotrophic prokaryote abundances were converted to C biomass using the factor 20 fg C bacterium^{-1} (Sime-Ngando et al. 1995). To calculate the volume of HF, these were considered to be spherical with a diameter of 2 µm for the size class of <3 µm (as most were around 2 µm), and mean diameters of 4 and 7.5 µm for the size classes 3−5 and 5−10 µm, respectively. The total C biomass of HF <10 µm was calculated using the factor 0.22 pg C µm^{-3} (Booth 1993). The volumes of ciliates <35 µm were calculated for each of the size classes by considering the ciliates to be spherical with a mean equivalent spherical diameter (ESD) of 12.5, 17.5, 22.5, 27.5, and 35 µm, for the size classes 10−15, 15−20, 20−25, 25−30, and 30−40 µm, respectively. The ciliate C biomass was estimated using the equation by Banchetti et al. (1989) using the factor 0.19 pg C µm^{-3}. The total microbial C biomass (µg C L^{-1}) was calculated as the sum of the C biomasses for all of these microorganisms. The Autotroph:Heterotroph (A:H) ratio of C biomass was calculated for each sample, assuming that the heterotrophic fraction corresponded to the sum of the C biomass of the heterotrophic prokaryotes, HF and ciliates, whereas the autotrophic part was represented by the phytoplankton Chl*a* biomass.

1.4. Estimating microorganism carbon flux depleted by juvenile oysters

Particulate fluxes were calculated for each planktonic component according to the following equations:

(1) $\Delta 0$ (µgC.lantern^{-1}. h^{-1}) = ([0]Tf –[0]T0)/(Tf-T0) × V

(2) Gross flux (µgC.lantern^{-1}. h^{-1}) = ([100, 200, 350]Tf – [0]T0)/(Tf-T0) × V

(3) Net flux (µgC.lantern^{-1}. h^{-1}) = (Gross flux - $\Delta 0$)

(4) Standardized flux (µg.DWg.h^{-1}) = Net flux/Total Dry Weight

Temporal variation of C biomass was calculated for each planktonic microbial component in absence (Equation 1: Lantern 0) and in presence (Equation 2: Lantern 100, 200, 350) of

juvenile oysters. V corresponded to the volume of the pelagic chamber containing the lantern. Gross fluxes measured in the absence of oysters (Equation 1) resulted from planktonic production and mortality, and from filtration of the epibionts (*Botryllus*) that began to colonize the lanterns from May. Epibiont biomass was not quantified during the experiment to avoid disturbing the lanterns, stressing the oysters, and any loss of decaying flesh. Moreover, epibiont biomass was negligible compared to oyster biomass. Equation 2 also integrates the influence of oysters on planktonic components, mainly through their filtration activity. Negative fluxes correspond to depletion while positive fluxes correspond to production. Postulating that abundance of planktonic organisms and epibionts did not vary initially according to oyster presence, net fluxes (Equation 3) obtained by subtracting fluxes observed in the presence (Lantern 100, 200, 350) and in the absence (Lantern 0) of juvenile oysters made it possible to exclusively highlight oyster interaction on planktonic components. Standardized fluxes correspond to net fluxes when corrected according to the Total Dry Weight of incubated oysters ($gDW.lantern^{-1}$). In the presence of oysters, negative net fluxes were interpreted as quantity of plankton depleted per hour and per lantern via oyster filtration without any precisions on ingestion or rejection pathways. It should be noted that we did not use the initial concentration of the planktonic microbial component in the presence of oysters ([100, 200, 350]T0) to calculate fluxes, since samples at T0 were taken after 25 minutes of pelagic chamber deployment and depletion had already begun. Use of [0]T0 in equation 2 prevents underestimation of the depleted biomass over time. Only net fluxes were presented since the objective of the study was to highlight the exclusive interaction of oyster juveniles on planktonic components during mortality events and according to density gradients, excluding the effect of epibionts on planktonic microbial components and the production, mortality and predation processes in the planktonic community in the absence of oysters.

1.5. Statistics

PERMANOVAs were used to test (i) the influence of juvenile oyster stocking Density (Dens 100, 200, 350), Week (W18 to W22) and their interaction (Week x Dens) on mortality and moribund oyster rates; (ii) weekly variations of OsHV-1 concentrations in oyster flesh and nutrients without the influence of oysters (lantern 0, T0: initial time) (iii) the effect of size Fraction, Week and their interaction on chlorophyll *a*, *b*, *c*, heterotrophic prokaryotes, HF and ciliates observed without the influence of oyster filtration (lantern 0, T0: initial time); (iv) the influence of juvenile oyster stocking Density (100, 200 or 350), Week and their interactions on fluxes of each planktonic microbial component and the A:H ratio. *A posteriori* tests were performed to compare the individual means with each other where there was significant variation. Linear correlations were tested between depletion and initial concentrations of each planktonic microbial component. Principal Component Analysis (PCA) was performed after normalisation of the whole dataset of planktonic microbial component biomasses at [0] T0 and on the whole dataset of net fluxes, i.e., PMC depletion observed in the presence of juvenile oysters corrected by the depletion observed in their absence. Analyses were carried out with JMP, PRIMER software and the PERMANOVA package (Plymouth Routines in Multivariate Ecological Research; Clarke and Warwick 2001).

2. Results

2.1. Mortality kinetic and characteristics of oyster juveniles

Mortality of juvenile oysters occurred in the Thau lagoon during April–May 2015. Instantaneous rates of mortality and moribund oysters varied significantly according to Week ($p = 0.001$, $n = 42$), but not according to Density (moribund $p = 0.6$, mortality $p = 0.9$, $n = 42$) or Week × Dens interaction (moribund $p = 0.9$, mortality $p = 0.4$, $n = 42$). The mortality episode started with the first observation of dead oysters at W17 (Fig. 2). Instantaneous

mortality rate increased from W17 to reach the highest mean at W19 (32 ± 3%; Fig. 2). This mortality peak was observed just after the observation of the highest rate of moribund oysters at W18 (32 ± 5%, Fig. 2). Mean instantaneous mortality rate significantly decreased from W20 to W22 and varied between 5.6 and 13.3% (Fig. 2). At the end of May 2015 (W22), the cumulative mortality rate reached 54.2 ± 1.1 %. Although the mortality rate seemed to be lower at higher density (350 < 200 < 100: 52.4%, 54.78%, 55.13%), this trend was not significant (Date: $p = 0.001$, Dens: $p = 0.16$, interaction $p = 0.8$, $n = 42$).

Oyster length and dry weight of flesh significantly varied with Week ($p < 0.0001$) and Density ($p < 0.0001$), with higher means for lower densities (100, 200 > 350). At W22, mean measurements (± SE) of juvenile oysters stocked at 100 ind.storey^{-1} were 34.2 ± 1.2 cm length, 3.44 ± 0.32 Total WWg, 81 ± 13 Flesh DWmg vs. 29.9 ± 1.44 cm length, 2.04 ± 0.24 Total WWg, 38 ± 12 DWmg at 350 ind.storey^{-1}. The total weight of oyster flesh per lantern varied significantly according to Week ($p = 0.0011$) and Density (< 0.0001) with higher means observed at 350 > 200 > 100. The lowest mean total flesh weight was observed at W16 for 100 (11.65 ± 0.73 DWg.lantern^{-1}) and the highest at W22 for 350 (50.03 ± 15.41 DWg.lantern^{-1}). In contrast to live juveniles oysters, the length of dead organisms did not vary according to the Week, with a mean of 22.33 ± 0.25 mm independently of the stocking Density.

During the mortality peak, 32% of oyster juveniles stocked in the experimental lanterns died, which, on the experimental scale, represented approximatively 8640 juveniles and 1.425 kg of decaying oyster flesh with a mean individual flesh weight of 0.16 WWg.

2.2. OsHV-1 quantification and histological assessment on oyster flesh

OsHV-1 DNA (C9C10 copies) was observed in oyster flesh and varied significantly according to the week in 2015 (log10 (x+1) p = 0.001, n = 83). OsHV-1 concentration (number of C9C10 copies per mg oyster) increased from W16 (1.50×10^{-03}) to W17 ($8.92 \times 10^{+01}$) to reach maximum values at W18 ($1.09 \times 10^{+04}$). It then decreased from W19 ($7.12 \times 10^{+03}$) to W20 ($7.79 \times 10^{+01}$), and was not detected in oyster flesh at W21. Based on the mortality and OsHV-1 detection results, five periods were defined as follows: "before" (W16) "starting" (W17), "moribund" (W18), "mortality peak (W19), "post-peak" (labelled 1, 2, 3 for W20, 21 and 22 respectively, Fig. 2).

Results of histological assessment showed that seven out of fifteen oysters contained ciliates (12 µm diameter, 23–32 µm length) in the pallial cavity and one had them on the gills during the W19 (Fig. 3).

2.3. Temporal variability of physical and chemical parameters and planktonic microbial components

All the following results correspond to sample analyses carried out in lantern 0 at T0 to highlight weekly variability of physical and chemical parameters and planktonic microbial components, without the direct influence from oysters.

Physical and chemical parameters

Temperature and salinity varied from 17 to 20.6°C and 35.3 to 36.35, respectively, during the experiment. In contrast to nitrate + nitrite and ammonium, phosphate varied significantly according to the Week ($NO_3 + NO_2$: p = 0.064; NH_4: p = 0.066; PO_4, p = 0.006, n = 12) with higher means observed in W18 and W22 (Fig. 4). High intra-week variability of NH_4 hid a trend of increasing NH_4 from W19 to W22. The N:P ratio was significantly different

according to the Week ($p = 0.018$, $n = 12$) with a lower mean observed at W18, i.e., during the "moribund" period (Fig. 4).

Autotrophic microorganisms

Total Chl*a* biomass was composed on average of 39.8% nano-fraction (3–20 µm). The contribution of picophytoplankton to Chl*a* biomass varied according to the Week, with higher contributions at W18 and W19 (33–40%) while microphytoplankton (>20 µm) contribution was maximal at W17 (41%) and W20 (55%, Fig. 4A). Total Chl*a* and total Chl*c* concentrations were significantly correlated ($r^2 = 0.95$, $n = 12$). Total Chl*a* and total Chl*c* concentrations varied significantly according to the Week following the same trend (Fig. 5A, B), with significant increases of total Chl*a* and total Chl*c* from W16 to W17 and a significant decrease from W20 to W22. In contrast, total Chl*b* concentration was not significantly correlated with Chl*a* ($r^2 = 0.32$, $n = 12$). The highest mean total Chl*b* was observed at W18 and W19 (Fig. 5C). Chl*a*, Chl*b* and Chl*c* varied significantly according to Fraction × Week interaction ($p = 0.001$, $n = 36$). Chl*c* was mainly composed of nano- and micro-phytoplankton (73–89%) in contrast to Chl*b*, which was mainly represented by the smaller fraction (0.7–3 µm: 45–82%, Fig. 5B, C) with higher means observed at W18 and W19, i.e., during the "moribund" and "mortality peak" periods. Picophytoplankton contribution to total phytoplankton biomass was higher during the "moribund" (39.5%) and "mortality" weeks (32.8%).

Heterotrophic microorganisms

Heterotrophic prokaryote abundance means varied from 2 to 4.5×10^6 mL^{-1} (Fig. 6A), but were not significantly different according to the Week ($p = 0.076$, $n = 12$). HF varied

significantly according to the Fraction × Week interaction ($p = 0.009$, $n = 24$). Total HF abundance was mainly represented by <3 and 3–5 µm fractions (88–100%, Fig. 6B). In contrast to <3 µm HF, 3–5 and >5 µm HF varied significantly according to the Week, with lower means observed at W18, i.e., the "moribund" period. Thus, total HF abundances were lower during the same period (Fig. 6B). Ciliates varied significantly according to the Fraction × Week interaction ($p = 0.0015$, $n = 59$). Total abundances of ciliates were higher in W18 and W19 than in W20, W17 or W22 (Fig. 6C). At W18, total ciliate abundances were mainly represented by the 10–25 µm size fraction encompassed by *Strombidium* sp., *Uronema* sp. and *Balanion* sp., which contributed 86% to total ciliate abundances. The week after (W19), however, the relative abundance of ciliates of 25–40 µm was higher, represented by *Strobilidium* sp. and *Lohmaniella* sp. (Fig. 6D), which contributed 60% to the total ciliate abundance. *Strombidium* sp., *Uronema* sp. and *Balanion* sp. were also observed in W19 but in lower abundances than in W18.

Previous results were synthetized by performing a PCA. The three weeks W17, W18 and W19 were separated from each other according to two components that explained 77% of the variability of initial conditions. W18 was opposed to W17 and showed a higher rate of moribund oysters, phosphate concentration and *Uronema* sp. abundance (Fig. 7A). W19 was separated from W17, with W18 as intermediate according to PC2, and showed the highest mortality rate, *Strobilidium* sp. and picophytoplankton biomasses.

2.4. Depletion of PMC by juvenile oysters

Fluxes of PMC studied in this investigation (heterotrophic prokaryotes, phytoplankton, heterotrophic flagellates, and ciliates) measured in the pelagic chambers containing juvenile

oysters were mainly negative. These trends were related to depletion over time, induced directly by juvenile oyster filtration or indirectly via trophic cascade.

Depletion of heterotrophic prokaryotes, phytoplankton and ciliates in the presence of juvenile oysters depended linearly on their initial concentration (Table 1). The most significant relationships were observed for the 3–20 µm size fraction, particularly for nanophytoplankton and ciliates of the 10–15 and 15–20 µm classes. For HF, only the relation with 3–5 µm was significant (Table 1).

The contribution of nano- (3–20 µm), micro- (>20 µm) and picophytoplankton (<3 µm) to the total depleted phytoplankton biomass in pelagic chambers containing juvenile oysters, varied per Week. The mean contribution of nano- and microphytoplankton represented 96.4% (2/3 and 1/3, respectively) of the total depleted phytoplankton biomass in the presence of oyster juveniles during the most of the studied weeks, with the exception of W17 and W18 when picophytoplankton (<3 µm) contribution increased, reaching 11.5 to 27.7%.

During these weeks, corresponding to the "starting" and "moribund" periods, the highest mean <3 µm-Chl*a* depletion was recorded, independentlty of the stocking densities (Fig. 8B). While depleted C biomasses of HF and ciliates were very low in comparison to depleted C biomass of total phytoplankton (see Y axis: Fig. 7A, B, C), negative fluxes were significant and varied per Week ($p = 0.001$), with higher depletion observed at W17 for HF (corresponding to 1.45% of depleted total phytoplankton: Fig. 8C) followed by higher depletion observed at W18 for ciliates (corresponding to 2% of depleted Total phytoplankton: Fig. 8D). A positive trend was observed according to oyster stocking density, with higher depletion observed at 100 than at 350 for most of the PMC and significant depletion for <3 µm phytoplankton ($p < 0.001$: 100, 200 < 350).

The PCA analysis resumed the results cited above (Fig. 7B). Depletion variability of PMC was mainly driven by *Uronema* sp., *Strobilidium* sp. and *Strombidium* sp. (PC1: 48.7%) and <3 µm picoplankton integrating picophytoplankton and HF (PC2: 23.4 % HF <3 µm: Fig.7B) with higher depletion of ciliates observed in W18 and higher depletion of picoplankton being observed in W17 and W18 than in W19. When PCA of initial conditions (Fig. 7A) and PMC depletion (Fig. 7B) were compared, results showed that in contrast to the main PMC (i.e. nano, HF 5-10, HF 3-5, Micro, *Uronema*), depletion of picophytoplankton (pico) and <3 µm HF are not correlated with initial biomass. Indeed, higher depletion of picophytoplankton was observed in W17 and W18 (Fig. 7B) while biomass was higher in W19 (Fig. 7A).

2.5. Influence of juvenile oysters on plankton biomass and trophic status

Autotrophic C biomass observed at final incubation time varied significantly according to Dens × Week interaction ($p < 0.0001$, $n = 40$). Autotrophic C biomass was significantly lower in presence than in absence of oyster juveniles (0 vs. 100, 200, 350 ind.storey^{-1}; Figure 9A) from W17 to W20. In contrast, heterotrophic C biomass did not vary significantly according to Density ($p = 0.135$, $n = 40$) or Dens × Week interaction ($p = 0.73$, $n = 40$). Indeed, heterotrophic C biomass did not vary according to the presence of juvenile oysters (Figure 9B). Juvenile oysters consumed higher biomass of autotrophic than heterotrophic C biomass, which comprised 97% heterotrophic prokaryotes. A:H C biomass observed at the final sampling time of incubation (Tf) varied significantly according to the Density of juvenile oysters ($p = 0.001$, $n = 40$), with a higher ratio observed in the absence of (0: 1.32 ± 0.17) rather than in the presence of juvenile oysters (100, 200, 350: 0.6 ± 0.03 : Fig. 9C) whatever the week (Week: $p = 0.06$, Dens × Week: $p = 0.26$, $n = 40$).

3. Discussion

Using an *in situ* approach, this study describes for the first time (i) changes in planktonic microbial components and (ii) influence of oyster juveniles on PMC and the trophic status of the Thau lagoon system in relation to a mortality episode of juvenile oysters.

3.1. Oyster mortality kinetic and magnitude

As expected, mortality of juvenile oysters occurred from the end of April until the beginning of May 2015 in the Thau lagoon. Seawater temperature ranged from 17 to 20.6°C during this period, which corresponds to with the classically observed temperature window of OsHV-1 viral infection (17–24°C, Pernet et al., 2012). In the present study, initial observations of dead oysters were made in W17 (21/04/15), followed by high abundances of moribund oysters in W18 (28/04/15), and the highest mortality peak in W19 (05/05/15). A symptom of moribund juveniles was valve-closing dysfunction, which appeared one week before their death. At the end of May (W22; 26/05/15), the cumulative mortality rate reached 54 ± 1 % with no significant differences among oyster juvenile stocking densities, simply a trend with lower mortality observed at high density (350 < 200 < 100). The kinetic and magnitude of mortality were comparable to those observed in 2015 and 2014 by the French RESCO network (http://wwz.ifremer.fr/observatoire_conchylicole: Fig. 10) for oyster juveniles stored in suspended bags. Pathogen analyses showed the presence of OsHV-1 in the flesh of moribund oysters from W17 with maximal values during moribund and mortality weeks, which confirmed OsHV-1 infection.

3.2. Temporal variability of nutrients and planktonic microbial components

In parallel to oyster mortality, temporal variability of nutrient concentrations and PMC were explored. Dissolved Inorganic Nitrogen (DIN), Phosphorus (DIP) and N:P ratio were low and consistent with those already observed in the Thau lagoon (Bec et al. 2005, Mostajir et al. 2015). The Thau lagoon was in N limitation according to the criteria of Justic et al. 1995 (DIN <1 µM and DIN/DIP <10), as already observed in spring (Bec et al. 2005). Increases of PO_4 and NH_4 were observed during the "moribund" and "mortality peak" periods. These relations resulted from leaching, followed by microbial mineralization of dead oyster tissue, as has been observed with decomposed mussels (Lomstein et al. 2006), jellyfish (West et al. 2009, Chelsky et al. 2016) or oyster (Richard et al. 2017). Indeed mineralization of dead oyster flesh was shown to induce huge increases of PO_4 (41 fold) and NH_4 (6 fold) fluxes at the water-dead oyster interface and a significant decrease of NH_4:PO_4 ratio in lab conditions (Richard et al. 2017). In the same way, DIN:DIP significantly decreased in the Thau lagoon during the "moribund" week (W18), reaching 2.6, which is lower than recorded during decomposition of oyster flesh in laboratory conditions (11.3: Richard et al. 2017). Richard et al. (2017) hypothesized that the disequilibria in ammonia and phosphorus releases in relation to flesh decomposition may favour bacterial proliferation. In the present study, abundances of heterotrophic prokaryotes ranged from 2 to 4.5 × 10^6 mL^{-1}, such as commonly observed in the Thau lagoon (Mostajir et al. 2015). While high intra-week variability was recorded, heterotrophic prokaryote abundances tended to increase from the beginning of follow-up to reach high abundances during the "Moribund" week, as expected. Decaying oyster tissues may stimulate the mineralization activity of heterotrophic prokaryotes inducing an increase in NH_4 concentration during the ensuing weeks. NH_4 may also be produced by excretion of living oysters (Mazouni 2004, Richard et al. 2017). The increase in excreted NH_4 may be induced by the increase in temperature, which simulates shellfish metabolism (Gosling et al. 2015), but also through the increase of oyster stocking biomass over the weeks, resulting from

the growth of surviving oysters. In contrast to NO_3 inputs, NH_4 releases are known to favour blooms of small rather than large-sized phytoplankton (Officer et al. 1982, Collos et al. 2003), in particular picophytoplankton (< 3 µm) bloom in coastal lagoons (Gilbert et al. 2010, Bec et al. 2011) as observed in this study. As expected, a bloom of picophytoplankton occurred during the follow-up. It began during the "starting" period (W17) and reached its highest concentrations during the "moribund" and "mortality peak" weeks (W18, W19). According to the high Chl*b* biomass observed in the 3-µm size fraction, picophytoplankton may be mainly comprised of Chlorophyta, Prasinophyceae and, more specifically, of the small (<1 µm) picoeukaryote *Ostreococcus tauri* (Chrétiennot-Dinet et al. 1995). *O. tauri* is known to be very abundant and represents the main component of the picophytoplankton community in the Thau lagoon (Vaquer et al. 1996, Bec et al. 2005). *O. tauri* populations, probably driven by nutrients, may also be partly regulated by HF (Kelly et al. 2003, Bec et al. 2005, Christaki et al. 2006). Total abundance of HF was low (97 to 215 mL^{-1}) in comparison to that previously reported in the Thau lagoon (Dupuy et al. 2000, Mostajir et al. 2015). HF abundances were mainly comprised of <5 µm size fraction. During the moribund period W18, HF recorded lower abundance, specifically for the >3 µm size fraction, which could be explained by predation exerted by ciliates. Indeed, huge abundances of ciliates <20 µm were observed during the "Moribund" period and reflected a massive proliferation of *Strombidium* sp., *Uronema* sp. and *Balanion* sp.. *Strombidium* sp. is known to grow on heterotrophic flagellates (Fenchel & Jonsson 1988), picoplankton-size particles (Christaki et al. 1998) and more specifically bacteria (Fenchel & Jonsson 1988) or prokaryotic autotrophs (Christaki et al. 1999). Taxa such as *Balanion* sp. (Aberle et al. 2007) and *Uronema* sp. are bacterivorous (Plunket & Hidu 1978, Christaki et al. 1998). Both the latter were highly correlated to the rate of moribund oysters. Ciliates were observed in the pallial cavity and the gills of moribund oyster juveniles (Fig. 3). Ciliates may proliferate in response to a bacterial proliferation

associated with decaying oyster tissue, as observed with *Uronema* sp. in cases of oyster mortality in nurseries or hatcheries (Plunket & Hidu 1978, Elston et al. 1999). The following week, proliferation of *Strobilidium* sp. was observed in relation to mortality rate, and as this ciliate is able to exert bacteriovory (Montagnes 1996), the decrease of heterotrophic prokaryote abundances might be explained by top-down control. After the mortality peak, ciliate abundances decreased progressively, becoming mainly constituted by *Strombidium* sp. This study shows, for the first time, that the structure of the planktonic microbial components changes within oyster mortality episode, with principal effects on picophytoplankton and ciliates.

3.3. Interactions of juvenile oysters with planktonic microbial components and changes on trophic status

Use of pelagic chambers enabled us to highlight the depletion of different PMC in the presence of juvenile oysters (Fig. 7B, 8). Like adult oysters (Barillé et al. 1993, Dupuy et al. 1999, 2000), juvenile oysters directly or indirectly consumed heterotrophic prokaryotes, phytoplankton, HF and ciliates. Depletion was linearly correlated with the initial concentration of most of the components, specifically for the 3–20 µm size fraction, particularly for nanophytoplankton, 10–20 µm ciliates and 3–5 µm HF (Table 1). Like adult oysters (Lam-Hoai et al. 1997, Dupuy et al. 2000, Mostajir et al. 2015), juveniles exert top-down control on PMC. Gills of commercial-sized-oysters (1.86 DWg) retain all >5 µm particles including flagellates, microphytoplankton, dinoflagellates, ciliates and large zooplankton. Only flagellates <5 µm and *O. tauri* are not very well retained (Dupuy et al. 2000). The authors underlined that microplanktonic primary producers were the main food source for adult oysters in the Thau Lagoon. The main food source for juvenile oysters during the study period was nanophytoplankton rather than microphytoplankton. In this study,

although nanophytoplankton represented 39% of total phytoplankton biomass, their mean contribution to total depleted autotrophic biomass by oyster juveniles was 60% (without considering W18 and W19). Our description of oyster juvenile interactions with PMC seems to be comparable with observations made on commercial-sized oysters (Dupuy et al. 2000, Mostajir et al. 2015). Nevertheless, in contrast to adults, this study showed that picophytoplankton and small heterotrophic flagellates (<3µm) were significantly depleted in the presence of oyster juveniles. Depletion of picoplankton did not depend on initial biomass; it occurred only at the start of the mortality episode (W17) and during the moribund period (W18), during which larger HF (W17) and ciliates (W18) were also depleted (Fig. 6 and 7). These observations could support the role of protozoa as a potential trophic link between picoplankton and filter-feeding bivalves (Le Gall et al. 1997, Dupuy et al. 1999, 2000). Our next investigation will be to examine pathogen fluxes and their relationships with planktonic components, focusing specifically on picoplanckton, HF and ciliates during starting and during moribund periods.

Biomass and abundance conversions of PMC in C biomass showed that juvenile oysters consumed higher biomass of autotrophic than heterotrophic C biomass (Fig. 9), which represented up to 97% of heterotrophic prokaryotes and 3% of ciliate and HF. The microbial Autotroph:Heterotroph C biomass (A:H) ratio allows us to define the status of PMC as autotrophic (>1) or heterotrophic (<1). Without oyster filtration, A:H in the present study ranged from 0.8 to 1.8, with a mean of 1.32 (Fig. 9), which corresponds to values observed in autumn in the Thau lagoon (A:H = 1.25) or in open ocean areas (A:H = 1.21, Mostajir et al. 2015). As previously observed during a mesocosm experimentation (Mostajir et al. 2015), the use of *in situ* pelagic chambers shows that oyster filtration induces a decrease in the structural A:H index (A:H = 0.6), indicating a trend towards a more heterotrophic microbial system. The process seemed to be accentuated after the mortality event, i.e., from W20, when

heterotrophic prokaryote abundances increased while ciliate abundances decreased, thus exerting a lower top-down control on heterotrophic prokaryote. In the Thau lagoon, heterotrophic conditions limited the metamorphosis success of *C. gigas* (Lagarde et al. 2017) which supports the idea that a shift toward heterotrophic system caused by filtration and mortality of oysters in excessive density may not favour sustainable development of shellfish culture.

4. Conclusions and perspectives

Through the use of innovative pelagic chambers, this *in situ* study shows for the first time (i) significant changes of planktonic microbial community structure during a mortality episode, with a proliferation of picoplankton and ciliates (*Balanion* sp., *Uronema* sp.) during the infection and mortality peak; (ii) that juvenile oysters mainly retained 3–20 µm plankton, with higher depleted biomass of autotrophic than heterotrophic microorganisms; iii) that filtration and mortality of juvenile oysters shifts the planktonic microbial structure towards a heterotrophic microbial system, where (iv), ciliates and HF may act as a trophic link between picoplankton and oysters. In contrast to adults, picophytoplankton and small heterotrophic flagellates (<3µm) were significantly depleted in the presence of oyster juveniles. Depletion of picoplankton occurred only at the starting of the mortality episode and during the moribund phase. The next stage in our investigation is to examine the effect of a mortality episode on pathogen fluxes in the water column, exploring their relationships with planktonic components and dead even non-living particles.

Acknowledgements

This work is a contribution to the MORTAFLUX program, funded by the Scientific Direction of Ifremer and by the EC2CO BIOHEFECT action (Coordinator: M. Richard). The

fellowships of C. Vanhuysse (Master II), C. Chantalat (Master I) and A. Degut (BSc) were funded by the MARBEC Research Unit and Ifremer. The authors thank C. Montagnani for discussions about methods of OsHV-1 analysis, and also D. McKenzie for his help in the field. Finally many thanks to Geneviève Guillouet and Zoely Rakotomonga-Rajaonah for their administrative help. We thank the "Bureau de Traduction de l'Université de Brest Occidentale" and "ACB-Ilo" for revising the English in the manuscript. Thanks to both anonymous reviewers for their detailed revision and very constructive and valuable comments on the previous versions of this manuscript.

References

Aberle N, Lengfellner K, Sommer U (2007) Spring bloom succession, grazing impact and herbivore selectivity of ciliate communities in response to winter warming. Oecologia 150:668–81

Aminot A, Kérouel R (2007) Dosage automatique des nutriments dans les eaux marines (Ifremer and Q MEDD, Eds.). Brest, 188 p.

Barbosa-Solomieu V, Miossec L, Vázquez-Juárez R, Ascencio-Valle F, Renault T (2004) Diagnosis of Ostreid herpesvirus 1 in fixed paraffin-embedded archival samples using PCR and in situ hybridisation. J Virol Methods 119:65–72

Barillé L, Prou J, Héral M, Bourgrier S (1993) No influence of food quality, but ration-dependent retention efficiencies in the Japanese oyster Crassostrea gigas. J Exp Mar Bio Ecol 171:91–106

Bayne B (2017) Feeding. In: Osborn P (ed) Developpement in Aquaculture and Fisheries Science, Vol. 41: Biology of oysters. Elsevier, Chippenham, UK, p 209–314

Bec B (2005) Phytoplankton seasonal dynamics in a Mediterranean coastal lagoon: emphasis on the picoeukaryote community. J Plankton Res 27:881–894

Bec B, Collos Y, Souchu P, Vaquer a, Lautier J, Fiandrino a, Benau L, Orsoni V, Laugier T (2011) Distribution of picophytoplankton and nanophytoplankton along an anthropogenic eutrophication gradient in French Mediterranean coastal lagoons. Aquat Microb Ecol 63:29–45

Bec B, Husseni-Ratrema J, Collos Y, Souchu P, Vaquer A (2005) Phytoplankton seasonal dynamics in a Mediterranean coastal lagoon: emphasis on the picoeukaryote community. J Plankton Res 27:881–894

Booth B (1993) Estimating cell concentration and biomass of autotrophic plankton using microscopy. In: Kemp F, Sherr B, Sherr E, Cole J (eds) Handbook of methods in aquatic microbial ecology. CRC Press, Boca Raton, FL., p 199–205

Callier MD, Richard M, McKindsey CW, Archambault P, Desrosiers G (2009) Responses of benthic macrofauna and biogeochemical fluxes to various levels of mussel biodeposition: An in situ "benthocosm" experiment. Mar Pollut Bull 58:1544–1553

Callier MD, Weise AM, McKindsey CW, Desrosiers G (2006) Sedimentation rates in a suspended mussel farm (Great-Entry lagoon, Canada): biodeposit production and dispersion. Mar Ecol Prog Ser:129–141

Chapelle A, Ménesguen A, Deslous-Paoli J-M, Souchu P, Mazouni N, Vaquer A, Millet B (2000) Modelling nitrogen, primary production and oxygen in a Mediterranean lagoon. Impact of oysters farming and inputs from the watershed. Ecol Modell 127:161–181

Chelsky A, Pitt KA, Ferguson AJP, Bennett WW, Teasdale PR, Welsh DT (2016) Decomposition of jellyfish carrion in situ: Short-term impacts on infauna, benthic nutrient fluxes and sediment redox conditions. Sci Total Environ 566-567:929–937

Chrétiennot-Dinet JM, Courties C, Vaquer A, Neveux J, Claustre H, Lautier J, Machado C (1995) A new marine picoeucaryote: *Ostreococcus tauri* gen. et sp. nov. (Chlorophyta, Prasinophyceae). Physiologica 34:285–292

Christaki U, Dolan JR, Pelegri S, Rassoulzadegan F (1998) Consumption of picophytoplankton-size particles by marine ciliates: Effects of physiological state of the ciliate and particle quality. Limnology 43:458–464

Christaki U, Jacquet S, Dolan JR, Vaulot D, Rassoulzadegan F (1999) Growth and grazing on *Prochlorococcus* and *Synechococcus* by two marine ciliates. Limnol Oceanogr 44:52–61

Christaki U, Vázquez-domínguez E, Courties C, Lebaron P (2006) Grazing impact of different heterotrophic nanoflagellates on eukaryotic (*Ostreococcus tauri*) and prokaryotic picoautotrophs (*Prochlorococcus* and *Synechococcus*). Environ Microbiol 7:1200–1210

Clarke KR, Warwick RM (2001) Changes in Marine Communities: An Approach to Statistical Analysis and Interpretation, 2nd Edition. PRIMER-E, Plymouth Marine Laboratory, UK

Collos Y, Vaquer A, Bibent B, Souchu P (2003) Response of coastal phytoplankton to ammonium and nitrate pulses: seasonal variations of nitrogen uptake and regeneration. Aquat Ecol:227–236

Corporeau C, Tamayo D, Pernet F, Quéré C, Madec S (2014) Proteomic signatures of the oyster metabolic response to herpesvirus OsHV-1 µVar infection. J Proteomics 109:176–87

Dupuy C, Gall S Le, Hartmann H, Bréret M (1999) Retention of ciliates and flagellates by the oyster *Crassostrea gigas* in French Atlantic coastal ponds: protists as a trophic link

between bacterioplankton and benthic suspension-feeders. Mar Ecol Prog Ser 177:165–175

Dupuy C, Vaquer A, Lam-Höai T, Rougier C, Mazouni N, Lautier J, Collos Y, Gall S Le (2000) Feeding rate of the oyster *Crassostrea gigas* in a natural planktonic community of the Mediterranean Thau Lagoon. Mar Ecol Prog Ser 205:171–184

Elston RA, Cheney D, Frelier P, Lynn D (1999) Invasive orchitophryid ciliate infections in juvenile Pacific and Kumomoto oysters , *Crassostrea gigas* and *Crassostrea sikamea*. Aquaculture 174:1–14

Fenchel T, Jonsson PR (1988) The functional biology of *Strombidium sulcatum*, a marine oligotrich ciliate (Ciliophora, Oligotrichina). Mar Ecol Prog Ser 48:1–15

Filgueira R, Guyondet T, Comeau LA, Grant J (2014a) Physiological indices as indicators of ecosystem status in shellfish aquaculture sites. Ecol Indic 39:134–143

Filgueira R, Guyondet T, Comeau LA, Grant J (2014b) A fully-spatial ecosystem-DEB model of oyster (*Crassostrea virginica*) carrying capacity in the Richibucto Estuary, Eastern Canada. J Mar Syst 136:42–54

Froján M, Arbones B, Zúñiga D, Castro C, Figueiras F (2014) Microbial plankton community in the Ría de Vigo (NW Iberian upwelling system): impact of the culture of *Mytilus galloprovincialis*. Mar Ecol Prog Ser 498:43–54

Gall S Le, Bel Hassen M, Gall P Le (1997) Ingestion of a bacterivorous ciliate by the oyster *Crassostrea gigas* : protozoa as a trophic link between picoplankton and benthic suspension-feeders. Mar Ecolgy Prog Ser 152:301–306

Garcia C, Thébault A, Dégremont L, Arzul I, Miossec L, Robert M, Chollet B, François C, Joly J, Ferrand S, Kerdudou N, Renault T (2011) Ostreid herpesvirus 1 detection and relationship with *Crassostrea gigas* spat mortality in France between 1998 and 2006. Vet Res 42:1–11

Gosling E (2015) How bivalves feed? In: Wiley J, Sons (eds) Marine Bivalve Molluscs. Wiley, John and Sons, p 99–144

Green TJ, Vergnes A, Montagnani C, Lorgeril J de (2016) Distinct immune responses of juvenile and adult oysters (*Crassostrea gigas*) to viral and bacterial infections. Vet Res 47:72

Jansen H, Strand Ø, Strohmeier T, Krogness C, Verdegem M, Smaal a (2011) Seasonal variability in nutrient regeneration by mussel Mytilus edulis rope culture in oligotrophic systems. Mar Ecol Prog Ser 431:137–149

Kelly CJO, Sieracki ME, Thier EC, Hobson IC (2003) A transient bloom of *Ostreococcus* (Chlorophyta, prasinophycea) in west neck bay, Long Island, New York. J phycol 39:850–854

Lagarde F, Roque E, Ubertini M, Mortreux S, Bernard I, Fiandrino A, Chiantella C, Bec B, Roques C, Bonnet D, Miron G, Richard M, Pouvreau S, Lett C (2017) Recruitment of the Pacific oyster *Crassostrea gigas* in a shellfish-exploited Mediterranean lagoon : discovery , driving factors and a favorable environmental window. Mar Ecol Prog Ser Ser 578:1–17

Lam-Hoai T, Rougier C, Lasserre G (1997) Tintinnids and rotifers in a northern Mediterranean coastal lagoon. Structural diversity and function through biomass estimations. Mar Ecol Prog Ser 152:13–25

Latasa M, Mora AG, Scharek R, Estrada M (2005) Estimating the carbon flux through main phytoplankton groups in the northwestern Mediterranean. 50:1447–1458

Mazouni N (2004) Influence of suspended oyster cultures on nitrogen regeneration in a coastal lagoon (Thau, Lagoon). Mar Ecol Prog Ser 276:103–113

Mineur F, Provan J, Arnott G (2014) Phylogeographical analyses of shellfish viruses: inferring a geographical origin for ostreid herpesviruses OsHV-1 (Malacoherpesviridae). Mar Biol 162:181–192

Montagnes DJS (1996) Growth responses of planktonic ciliate in the genera *Strobilidium* and *Strombidium*. Mar Ecol Process Ser 130:241–254

Mostajir B, Roques C, Bouvier C, Bouvier T, Fouilland É, Got P, Floc'h E Le, Nouguier J, Mas S, Sempéré R, Sime-Ngando T, Troussellier M, Vidussi F (2015) Microbial food web structural and functional responses to oyster and fish as top predators. Mar Ecol Prog Ser 535:11–27

Neveux J, Lantoine F (1993) Spectrofluorometric assay of chlorophylls and phaeopigments using the least squares approximation technique. Deep Res 40:1747–1765

Officer CB, Smayda TJ, Mann R (1982) Benthic filter feeding : a natural eutrophication control. Mar Ecol Prog Ser 36:225–236

OIE World Organisation for Animal Health (2018) Section 2.4. Diseases of Molluscs, Chapter 2.4.0. General information, 2.4. Histological techniques. In: Manual of Diagnostic Tests for Aquatic Animals.p 4–6

Pernet F, Barret J, Gall P Le, Corporeau C, Dégremont L, Lagarde F, Pépin J, Keck N (2012) Mass mortalities of Pacific oysters *Crassostrea gigas* reflect infectious diseases and vary with farming practices in the Mediterranean Thau lagoon, France. Aquac Environ Interact 2:215–237

Plunket L, Hidu H (1978) The role of *Uronema marinum* (Protozoa) in oyster production. Aquaculture 15:219–225

Richard M, Archambault P, Thouzeau G, Desrosiers G (2006) Influence of suspended mussel lines on the biogeochemical fluxes in adjacent water in the Îles-de-la-Madeleine (Quebec, Canada). Can J Fish Aquat Sci 63:1198–1213

Richard M, Archambault P, Thouzeau G, McKindsey CW, Desrosiers G (2007) Influence of suspended scallop cages and mussel lines on pelagic and benthic biogeochemical fluxes in Havre-aux-Maisons Lagoon, Îles-de-la-Madeleine (Quebec, Canada). Can J Fish Aquat Sci 64:1491–1505

Richard M, Bourreau J, Montagnani C, Ouisse V, Gall P Le, Fortune M, Munaron D, Messiaen G, Callier MD, Roque E (2017) In fluence of OSHV-1 oyster mortality episode on dissolved inorganic fluxes : An ex situ experiment at the individual scale. Aquaculture 475:40–51

Robert P, McKindsey CW, Chaillou G, Archambault P (2013) Dose-dependent response of a benthic system to biodeposition from suspended blue mussel (*Mytilus edulis*) culture. Mar Pollut Bull 66:92–104

Sime-Ngando T, Gosselin M, Roy S, Chanut J-P (1995) Significance of planktonic ciliated protozoa in the Lower St . Lawrence Estuary : comparison with bacterial , phytoplankton , and particulate organic carbon. Aquat Microb Ecol 9:243–258

Smaal AC, Schellekens T, Stralen MR van, Kromkamp JC (2013) Decrease of the carrying capacity of the Oosterschelde estuary (SW Delta, NL) for bivalve filter feeders due to overgrazing? Aquaculture 404-405:28–34

Souchu P, Vaquer A, Collos Y, Landrein S, Deslous-paoli J-M, Bibent B (2001) Influence of shellfish farming activities on the biogeochemical composition of the water column in Thau lagoon. Mar Ecol Prog Ser 218:141–252

Tamayo D, Corporeau C, Petton B, Quere C, Pernet F (2014) Physiological changes in Pacific oyster *Crassostrea gigas* exposed to the herpesvirus OsHV-1µVar. Aquaculture 432:304–310

Tamburri MN, Zimmer-Faust RK (1996) Suspension feeding: Basic mechanisms controlling recognition and ingestion of larvae. Limnol Oceanogr 41:1188–1197

Troost K, Kamermans P, Wolff WJ (2008) Larviphagy in native bivalves and an introduced oyster. J Sea Res 60:157–163

Trottet A, Roy S, Tamigneaux E, Lovejoy C, Tremblay R (2008) Impact of suspended mussels (*Mytilus edulis* L.) on plankton communities in a Magdalen Islands lagoon (Québec, Canada): A mesocosm approach. J Exp Mar Bio Ecol 365:103–115

Utermöhl H (1958) Zur Vervollkommnung der quantitativen Phytoplankton-Methodik. Mitt int Ver theor angew Limnol 9:1–38

Vaquer A, Troussellier M, Courties C, Bibent B (1996) Standing stock and dynamics of picophytoplankton in the Thau Lagoon (northwest Mediterranean coast). Limnol Ocean 41:1821–1828

Vidussi F, Mostajir B, Fouilland E, Floc'h E Le, Nouguier J, Roques C, Got P, Thibault-Botha D, Bouvier T, Troussellier M (2011) Effects of experimental warming and

increased ultraviolet B radiation on the Mediterranean plankton food web. Limnol Oceanogr 56:206–218

West EJ, Welsh DT, Pitt KA (2009) Influence of decomposing jellyfish on the sediment oxygen demand and nutrient dynamics. Jellyfish Bloom 616:151–160

Table 1 Results of linear regression between net fluxes (equation 3), ie. fluxes observed in pelagic chambers containing oysters (100, 200, 350 ind.storey^{-1}), corrected by fluxes observed in control pelagic chambers (0) (µg C. PelagicChamber^{-1}.h^{-1}), and initial concentration (0 T0: µgC. L^{-1}) of each studied planktonic microbial components (PMC: i.e., heterotrophic prokaryote, phytoplankton, HFs and ciliates and according to size fraction. Slope indicates the sign of the relationship (+ or -), R^2: determination coefficient, n: number of observation, p: probability value. $p < 0.05$: *; $p < 0.01$: **, $p < 0.001$: *** Bold characters show the most significant relations.

Net Fluxes vs. **Concentration of PMC**	**Initial**	**slope**	**R^2**	**n**	**p**	
Heterotrophic prokaryote		-	0.49	30	< 0.0001	***
Total Phytoplankton		-	0.60	30	< 0.0001	***
	< 3 µm		0.07	30	0.1613	
	3-20 µm	**-**	**0.76**	**30**	**< 0.0001**	***
	> 20 µm	-	0.20	30	0.0121	*
Total Ciliate			0.02	12	0.6438	
	10-15 µm	**-**	**0.80**	**12**	**< 0.0001**	***
	15-20 µm	**-**	**0.89**	**12**	**< 0.0001**	***
	20-25 µm	-	0.34	12	0.045	*
	25-30 µm		0.30	12	0.0651	
Total Flagellate			0.21	12	0.1389	
	< 3 µm		0.18	12	0.17	
	3-5 µm	**-**	**0.87**	**12**	**< 0.0001**	***
	5-10 µm		0.01	12	0.8043	

Figure 1: A) Experimental design, consisting of 4 juvenile oyster stocking density conditions (0, 100, 200, 350 ind.storey^{-1}), 6 weeks and 2 sampling times (T0: initial time, Tf: final time). Conditions were replicated twice. N = 96 data, B) Schema and photo of Pelagic chamber composed of a cylindrical tube, a waterproof cap, a water circulation system driven by an autonomous pump, and an optode oxygen probe.

Figure 2: Mean (± SE) instantaneous rates of moribund oysters and mortality observed according to sampling week (W16: 13-19th April, W17 : 20-26 th April, W18 : 27 th April-3 th May, W19 : 4-10 th May, W20 : 11-17 th May, W21: 18-24th May and W22 : 25-31 th May 2015) whatever the juvenile oyster stocking density. Different lower and capital letters indicate significant differences among weeks for moribund and mortality rates, respectively.

Figure 3: Transverse histological sections of a juvenile oyster collected the 5th May 2015, showing ciliates within the pallial cavity. Size is indicated by the bars (µm). Analyses (15.05.0021A.001a) were realized by the Histalim laboratory, Montpellier, France.

Figure 4: Mean (± SE) ammonium (NH_4), nitrate + nitrite (NO_3 + NO_2), phosphate (PO_4) concentrations and N:P ratio observed at T0 without direct influence of oysters (Lantern 0) according to sampling week (W16: 13-19th April, W17 : 20-26 th April, W18 : 27 th April-3 th May, W19 : 4-10 th May, W20 : 11-17 th May, W21: 18-24th May and W22 : 25-31 th May 2015).

Figure 5: Mean (± SE) A) Chl*a*, B) Chl*c* and C) Chl*b* concentrations observed at T0 without direct influence of oysters (Lantern 0) according to size fraction (< 3, 3–20, > 20 µm) and sampling week (W16: 13-19th April, W17 : 20-26 th April, W18 : 27 th April-3 th May, W19 : 4-10 th May, W20 : 11-17 th May, W21: 18-24th May and W22 : 25-31 th May 2015). Different capital and lower case letters indicate significant difference among weeks for total and <3µm Chl biomass, respectively.

Figure 6: Mean (± SE) A) heterotrophic prokaryotes (10^6.mL^{-1}, B) flagellates (ind.ml^{-1}) and C) ciliates (ind.L^{-1}) abundances observed at T0 without direct influence of oysters (Lantern 0) according to size fraction (A: < 3; 3–5; 5–10 µm, B: 10–15; 15–20; 20–25; 25–30; 30–40 µm), D) ciliate genus and sampling weeks (W16: 13-19th April, W17 : 20-26 th April, W18 : 27 th April-3 th May, W19 : 4-10 th May, W20 : 11-17 th May, W21: 18-24th May and W22 : 25-31 th May 2015) . Different capital letters indicate a significant difference among weeks for total abundance of flagellates and ciliates.

Figure 7: PCA of A) Initial conditions (Lantern 0, T0) integrating rates of mortality and moribund oysters, concentrations of nutrients (NH_4, PO_4), and carbon biomasses of MFW components (heterotrophic prokaryote (HP), phytoplankton: pico (0–3 µm), nano (3–20 µm), micro (>20 µm), more abundant ciliate species (*Strombidium* sp., *Uronema* sp., *Strobilidium* sp., *Balanion* sp.) and different Heterotrophic Flagellate (HF) size fractions (< 3, 3–5, 5–10 µm) and B) depletion of the latter MFW components observed in the presence of juvenile oysters and corrected by depletion observed in absence of juvenile oysters, observed according to week (W17 : 20-26 th April, W18 : 27 th April-3 th May, W19 : 4-10 th May) during which database was completed. Highest eigenvalues were attributed to bold parameters on PC1 and underlined ones on PC2.

Figure 8: Mean (± SE) fluxes observed in pelagic chambers containing oysters, corrected by fluxes observed in the control lantern (0), and reported per unit of oyster biomass contained in chambers (µgC.gDW^{-1}.h^{-1}) for biomass of A) picophytoplankton (Chla < 3 µm) , B) flagellates, and C) ciliates, measured according to sampling Week (W16: 13-19th April, W17 : 20-26 th April, W18 : 27 th April-3 th May, W19 : 4-10 th May, W20 : 11-17 th May, W21: 18-24th May and W22 : 25-31 th May 2015) and stocking Density (100, 200, 350 ind.storey^{-1}).

Figure 9: Mean (± SE) A) Autotrophic, B) Heterotrophic Carbon Biomass (µg C L^{-1}) and C) Autotrophic : Heterotrophic Ratio (A:H) observed at Tf according to sampling Week (W16:

13-19th April, W17 : 20-26 th April, W18 : 27 th April-3 th May, W19 : 4-10 th May, W20 : 11-17 th May, W21: 18-24th May and W22 : 25-31 th May 2015) and stocking Density (0, 100, 200, 350 ind.storey^{-1}). Stars indicate a significant difference of carbon biomass or ratio among juvenile oyster Densities within Week in contrast to the horizontal line.

Figure 10: Comparison of mean (± SE) cumulative mortality rates of oyster juveniles observed in the Thau lagoon in this study (2015) compared with those observed by the RESCO networks in 2014 and 2015.

FIGURES

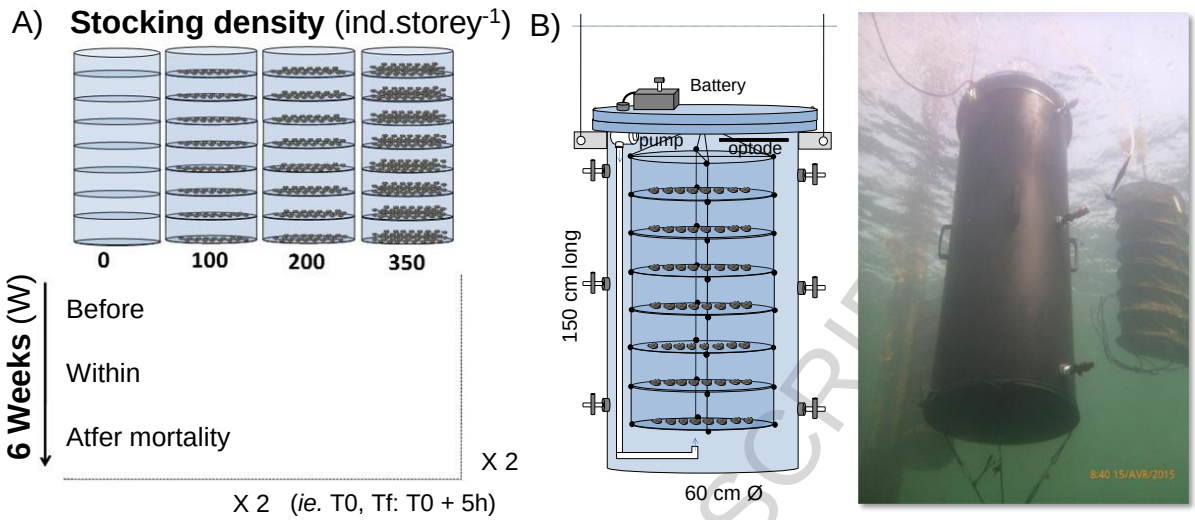

Figure 1. Richard et al.

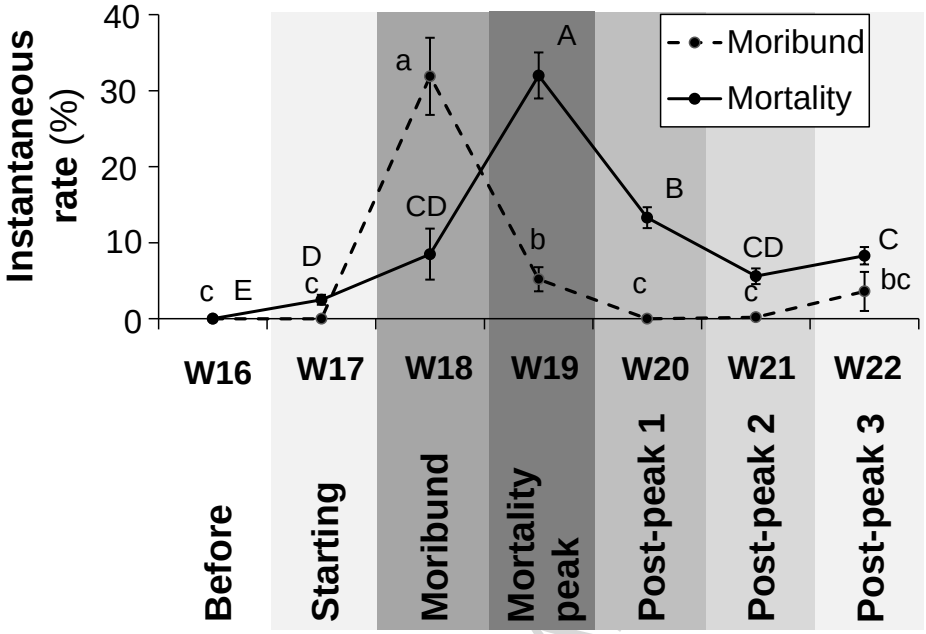

Figure 2. Richard et al.

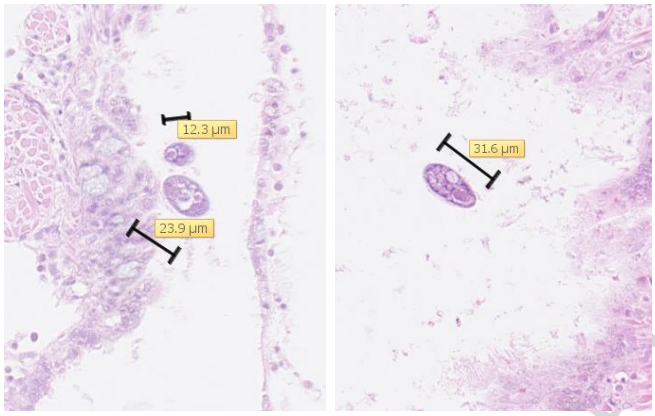

Figure 3. Richard et al.

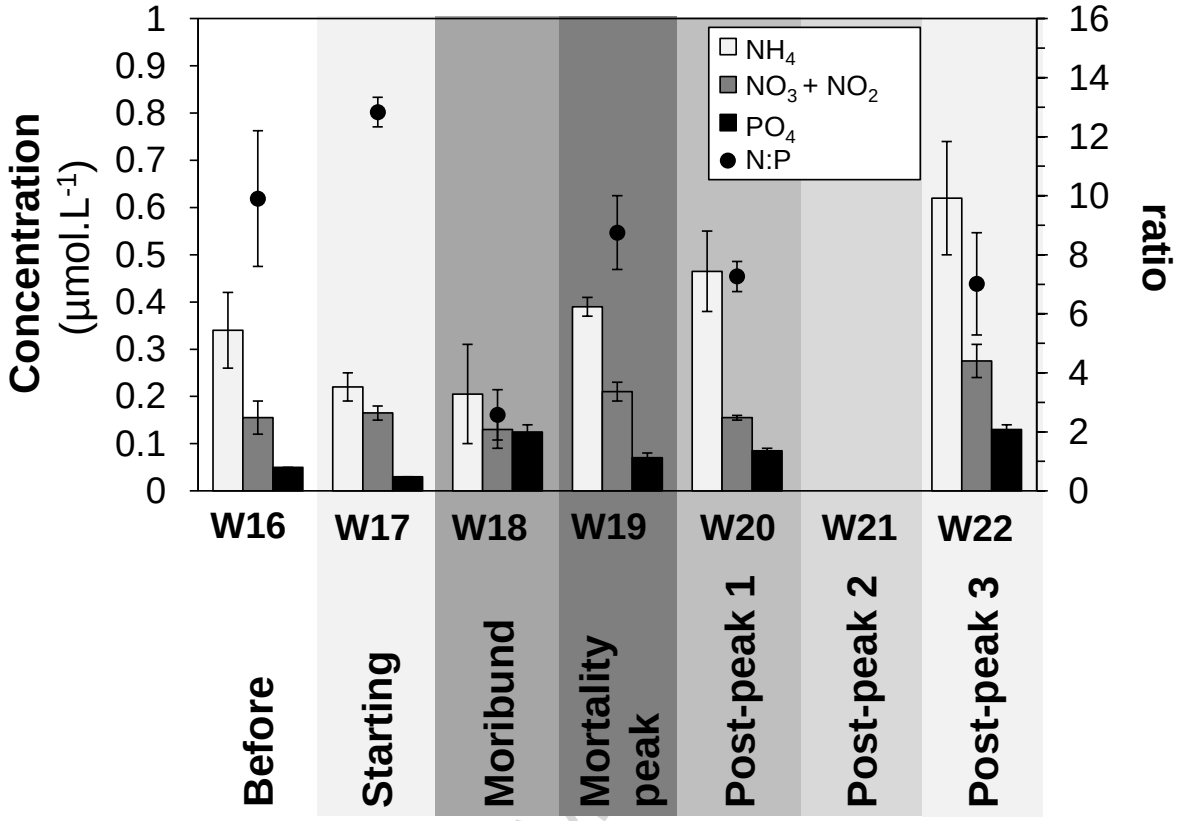

Figure 4. Richard et al.

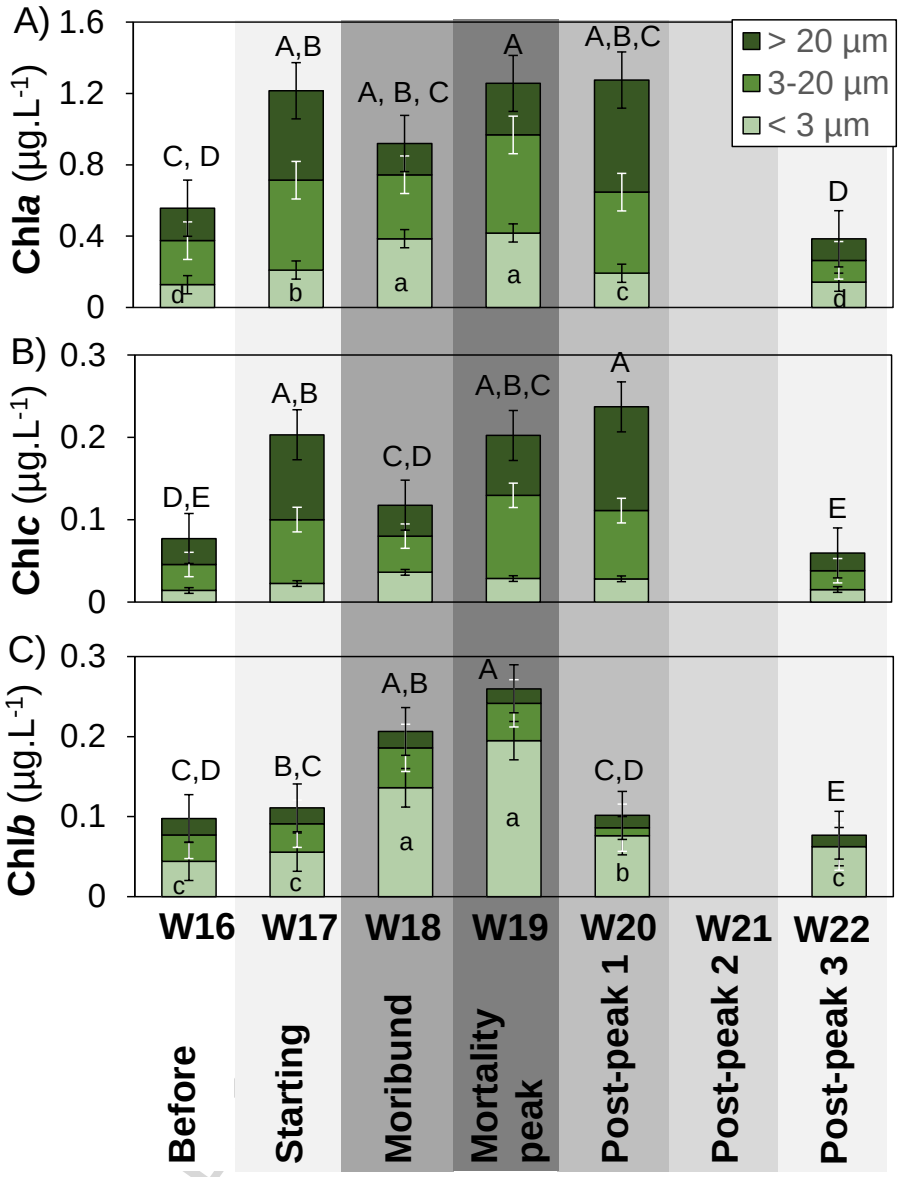

Figure 5. Richard et al.

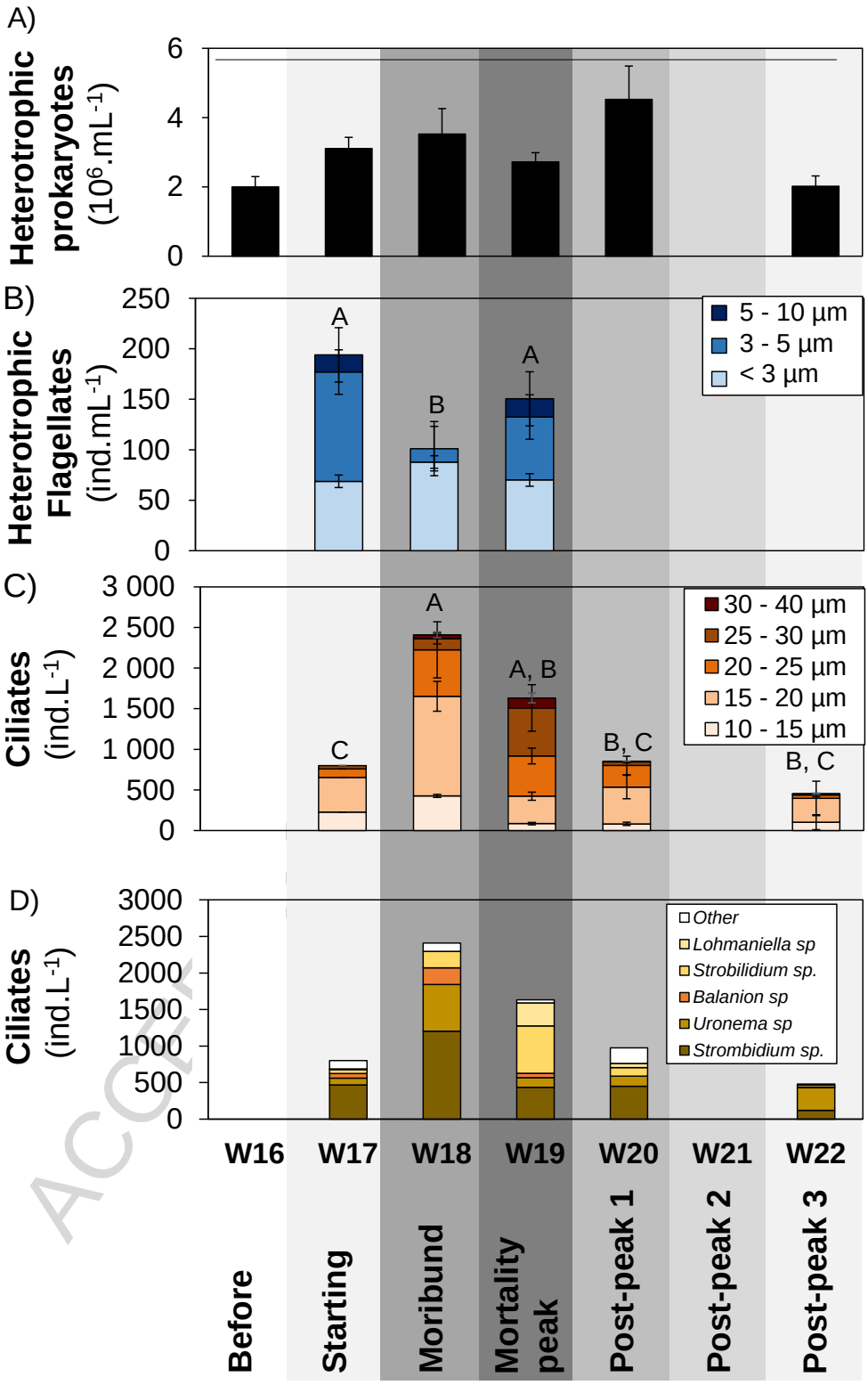

Figure 6. Richard et al.

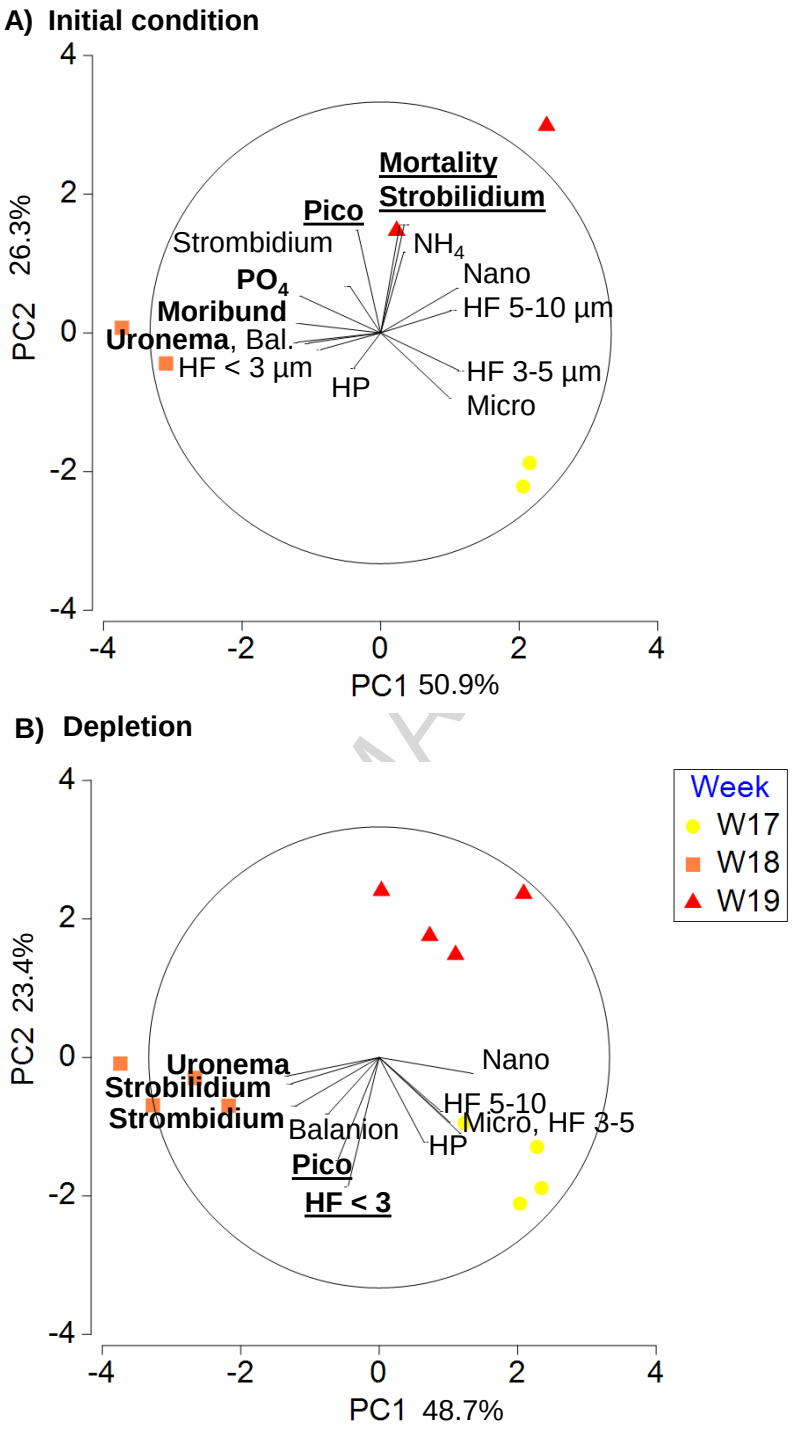

Figure 7. Richard et al.

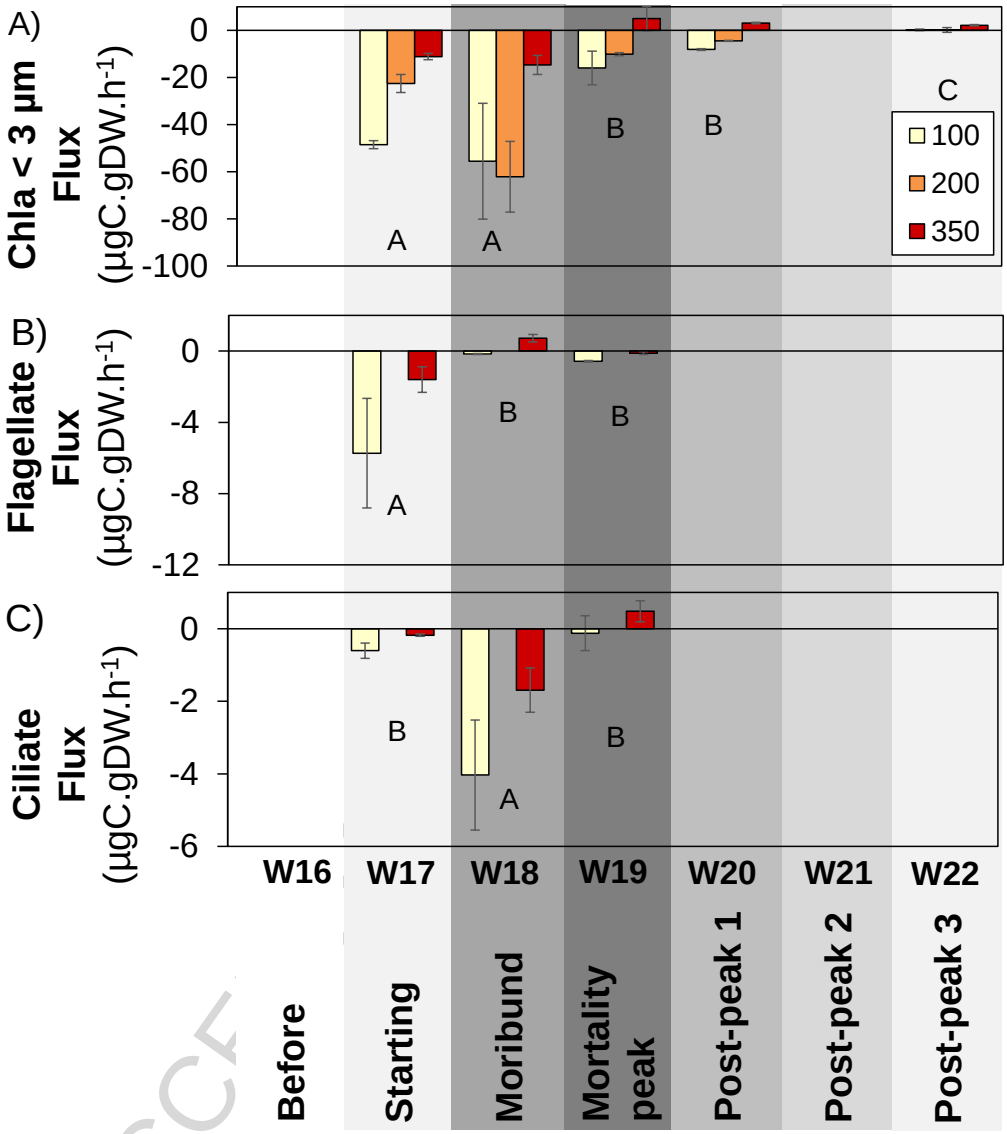

Figure 8. Richard et al.

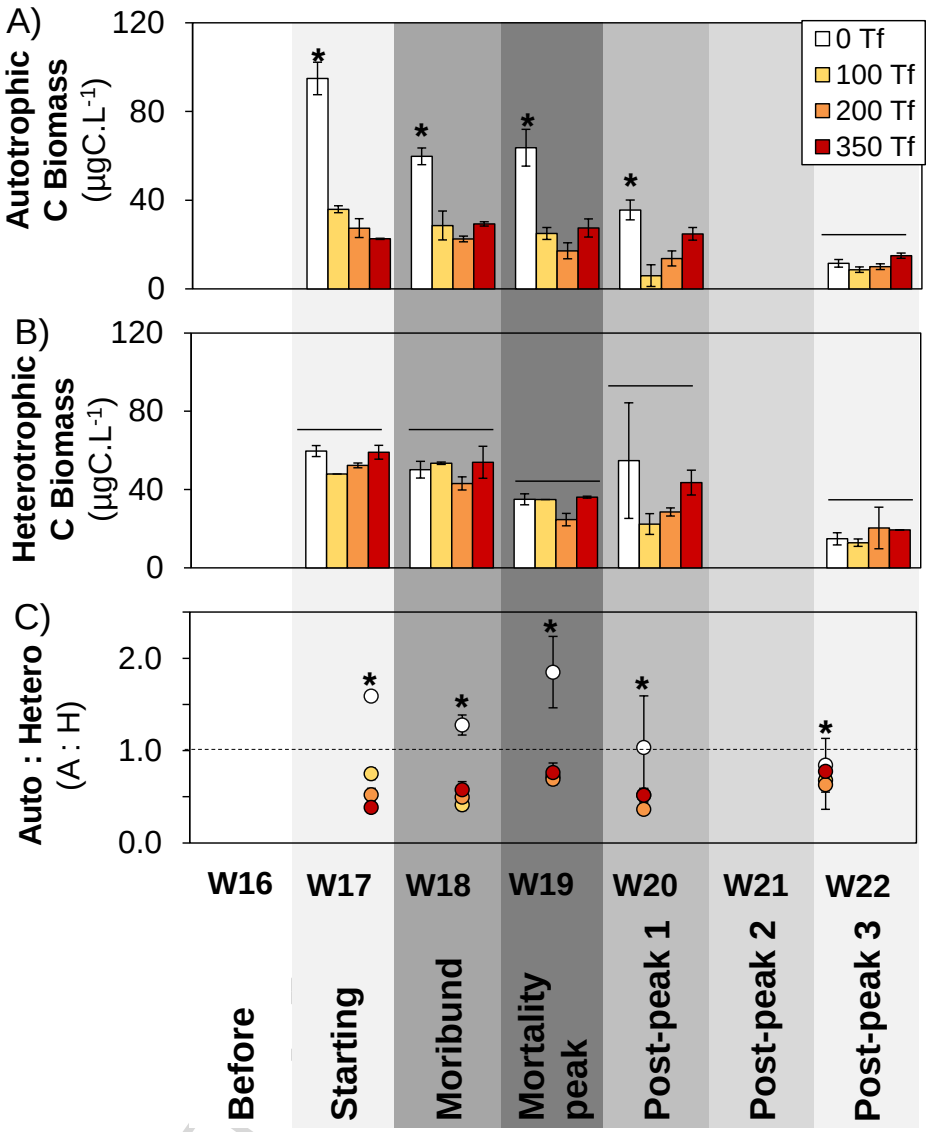

Figure 9. Richard et al.

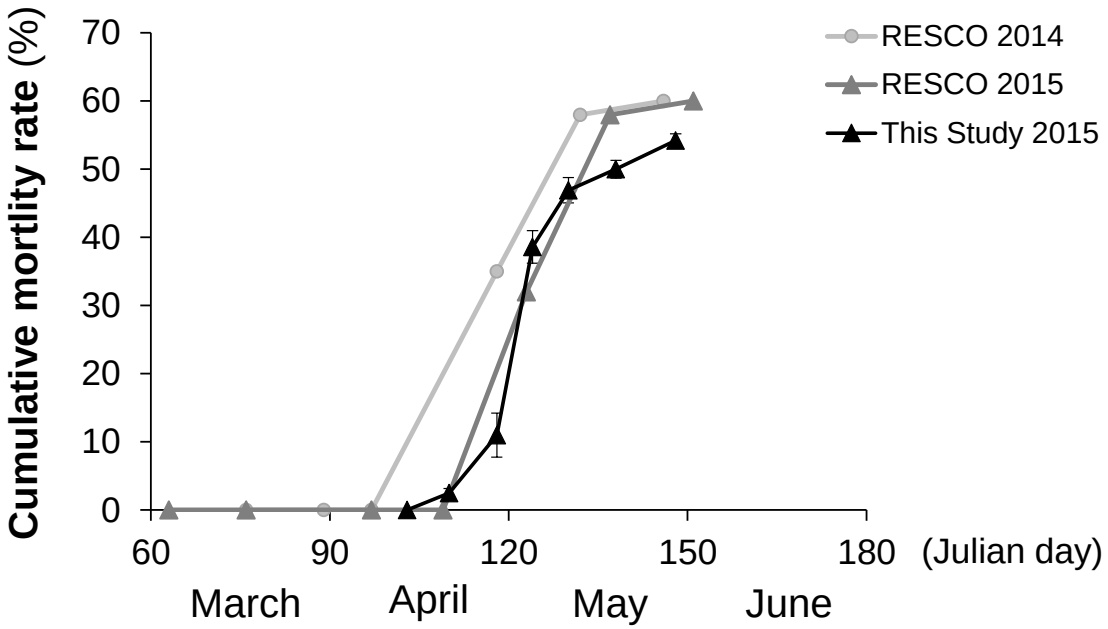

Figure 10. Richard et al.

HIGHLIGHTS

- The planktonic microbial components (PMC) change during OsHV-1 oyster juvenile mortality
- Picophytoplankton and ciliates increase during infection and mortality periods
- Filtration and mortality of juvenile oysters shift PMC toward a heterotrophic system

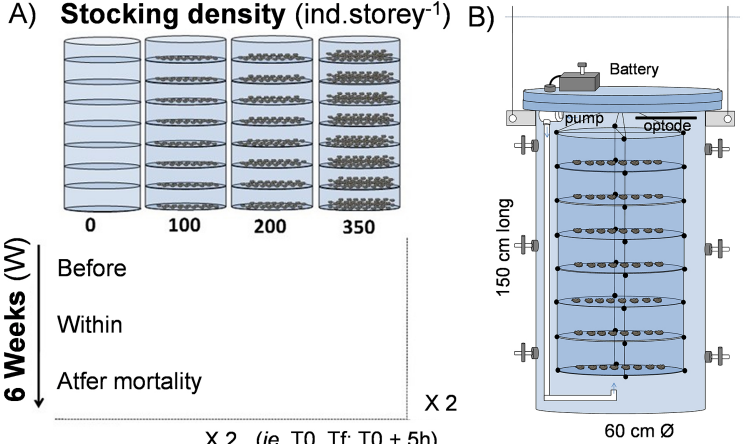
A)
Stocking density (ind.storey-1)
0
100
200
350
6 Weeks (W)
Before
Within
Atfer mortality
X 2
X 2 (ie. T0, Tf: T0 + 5h)
B)
Battery
pump
optode
150 cm long
60 cm Ø
8:40 15/AVR/2015

Figure 1

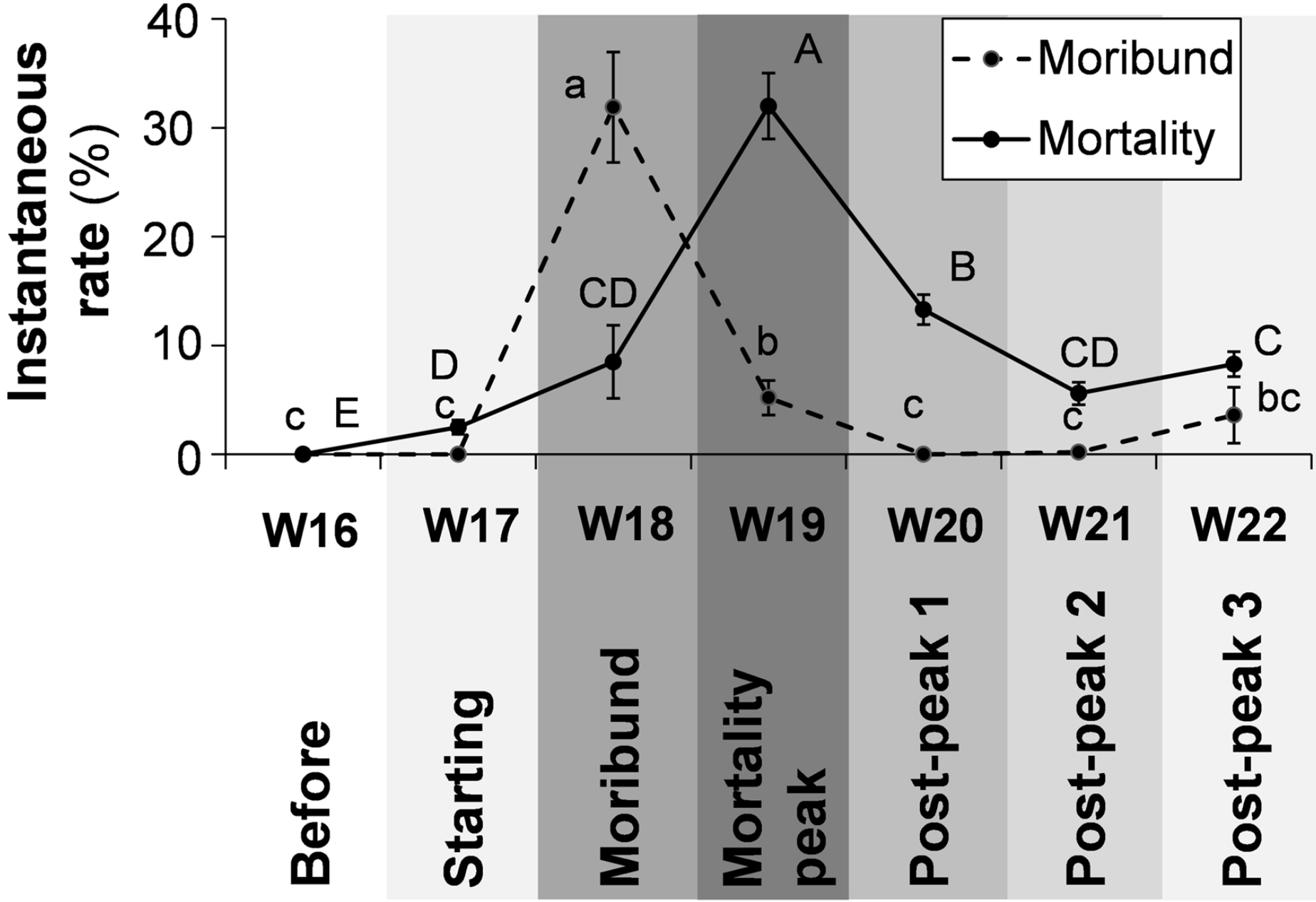
Instantaneous rate (%)
40
30
20
10
0
Moribund
Mortality
a
A
CD
B
D
b
CD
C
c
E
c
c
c
c
bc
W16
W17
W18
W19
W20
W21
W22
Before
Starting
Moribund
Mortality peak
Post-peak 1
Post-peak 2
Post-peak 3

Figure 2

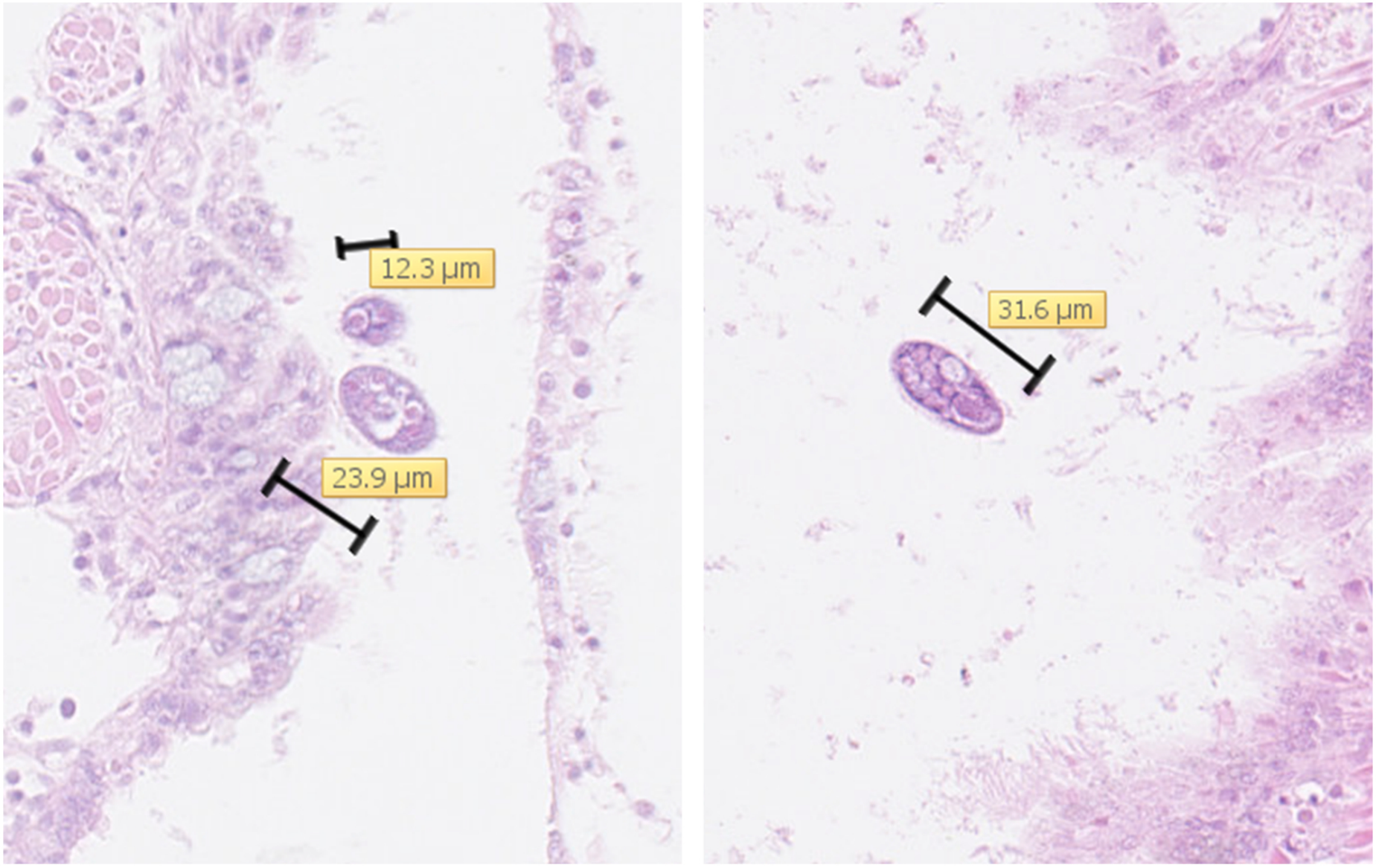

Figure 3

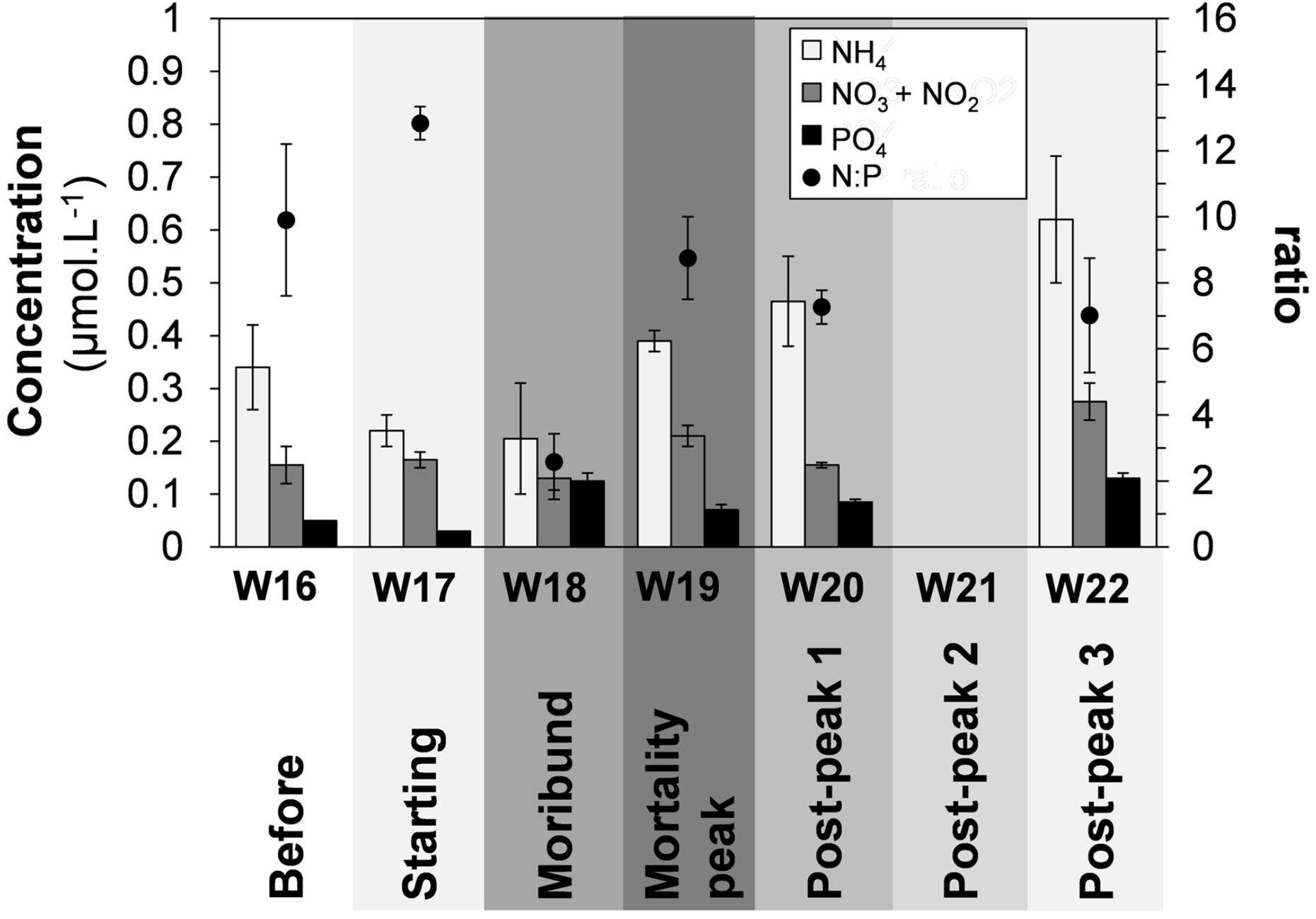
Concentration
(µmol.L-1)
1
0.9
0.8
0.7
0.6
0.5
0.4
0.3
0.2
0.1
0
16
14
12
10
8
6
4
2
0
ratio
NH4
NO3 + NO2
PO4
N:P
W16
W17
W18
W19
W20
W21
W22
Before
Starting
Moribund
Mortality peak
Post-peak 1
Post-peak 2
Post-peak 3

Figure 4

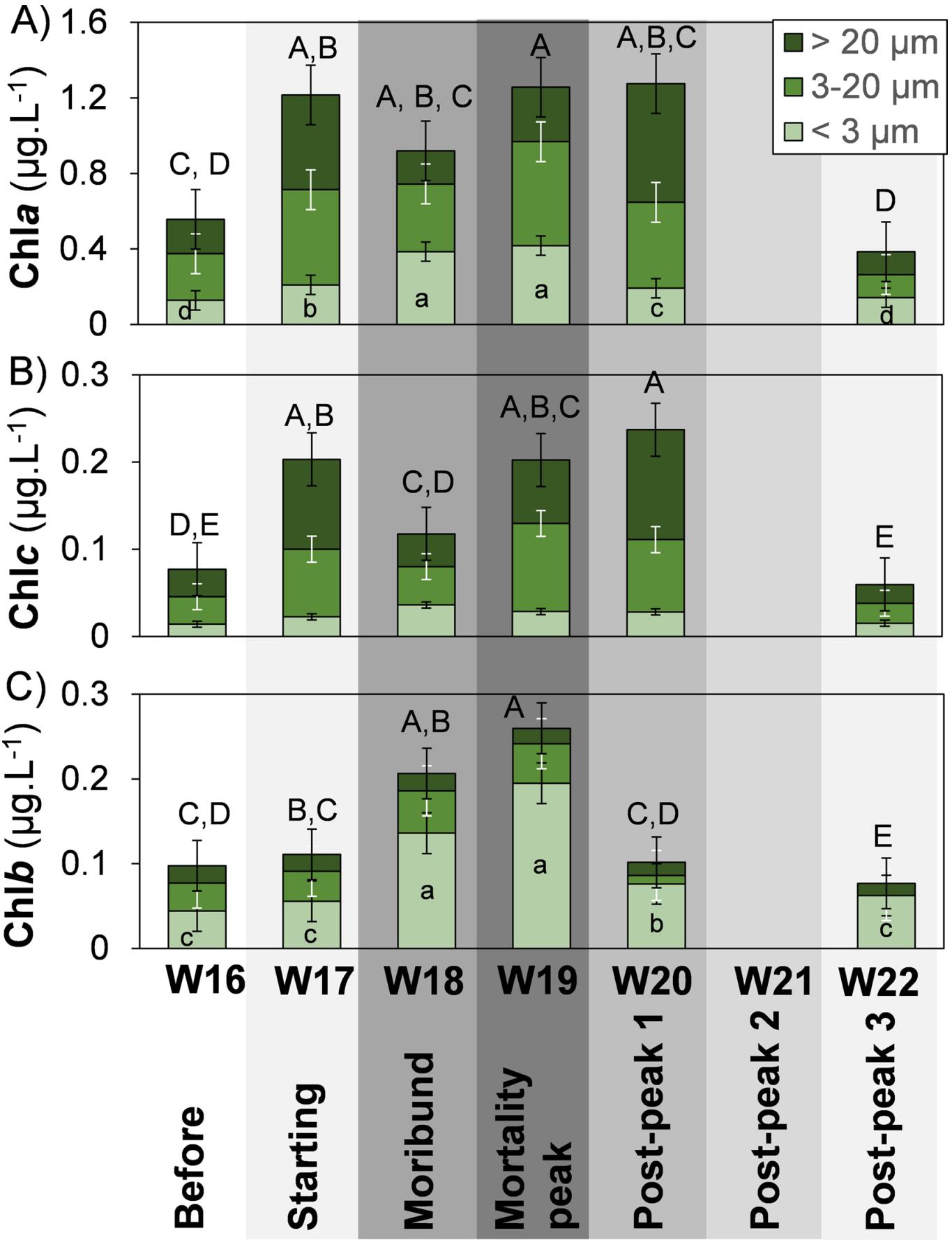
A)
Chla (µg.L-1)
1.6
1.2
0.8
0.4
0
> 20 µm
3-20 µm
< 3 µm
C, D
A,B
A, B, C
A
A,B,C
D
d
b
a
a
c
d
B)
Chlc (µg.L-1)
0.3
0.2
0.1
0
D,E
A,B
C,D
A,B,C
A
E
C)
Chlb (µg.L-1)
0.3
0.2
0.1
0
C,D
B,C
A,B
A
C,D
E
c
c
a
a
b
c
W16
W17
W18
W19
W20
W21
W22
Before
Starting
Moribund
Mortality peak
Post-peak 1
Post-peak 2
Post-peak 3

Figure 5

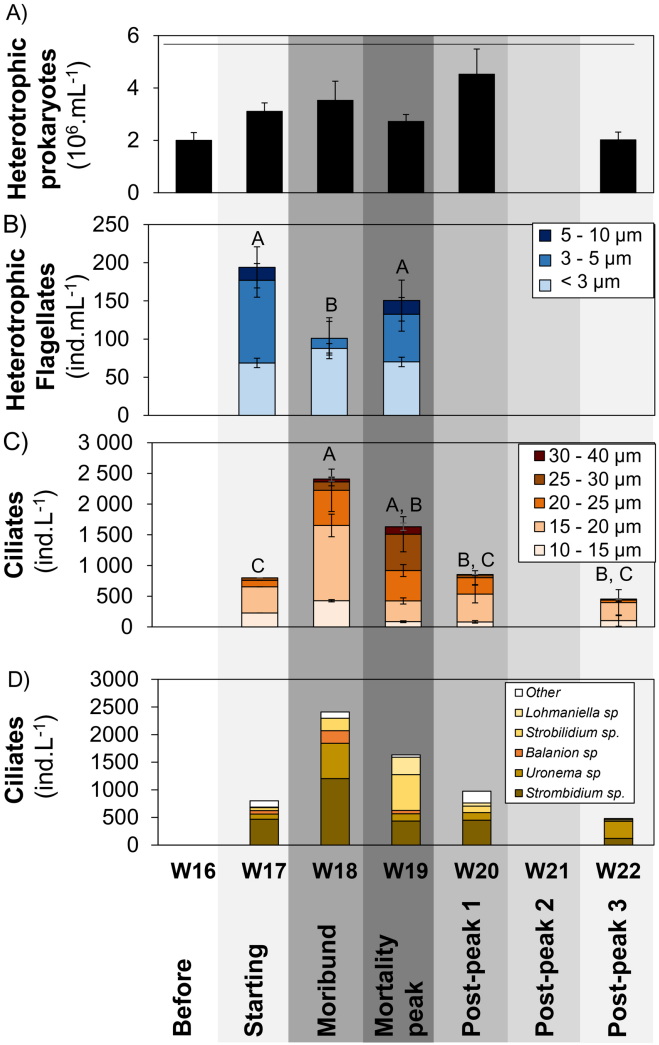
A)
Heterotrophic prokaryotes (10^6.mL^-1)
6
4
2
0
B)
Heterotrophic Flagellates (ind.mL^-1)
250
200
150
100
50
0
A
B
A
5 - 10 µm
3 - 5 µm
< 3 µm
C)
Ciliates (ind.L^-1)
3 000
2 500
2 000
1 500
1 000
500
0
C
A
A, B
B, C
B, C
30 - 40 µm
25 - 30 µm
20 - 25 µm
15 - 20 µm
10 - 15 µm
D)
Ciliates (ind.L^-1)
3000
2500
2000
1500
1000
500
0
Other
Lohmaniella sp
Strobilidium sp.
Balanion sp
Uronema sp
Strombidium sp.
W16
W17
W18
W19
W20
W21
W22
Before
Starting
Moribund
Mortality peak
Post-peak 1
Post-peak 2
Post-peak 3

Figure 6

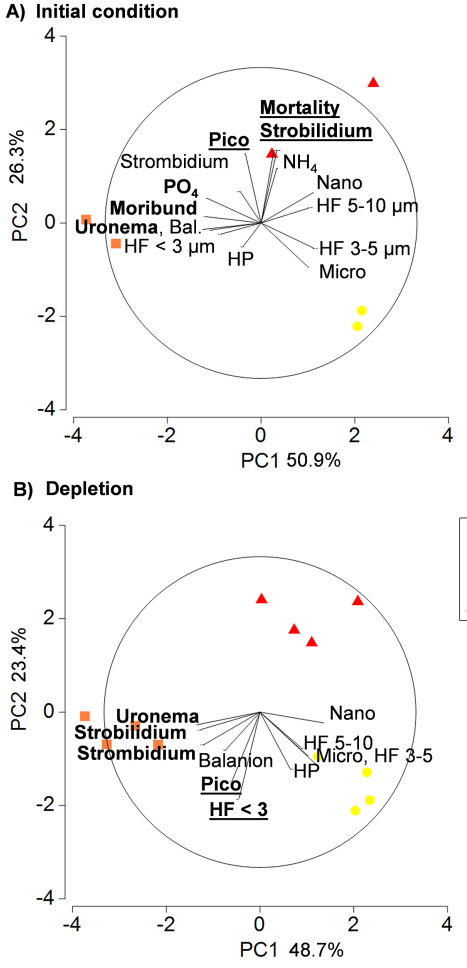
A) Initial condition
Mortality
Strobilidium
Pico
Strombidium
NH4
PO4
Nano
Moribund
HF 5-10 µm
Uronema, Bal.
HF < 3 µm
HF 3-5 µm
HP
Micro
PC2 26.3%
PC1 50.9%
B) Depletion
Week
W17
W18
W19
Uronema
Strobilidium
Strombidium
Nano
HF 5-10
Micro, HF 3-5
Balanion
HP
Pico
HF < 3
PC2 23.4%
PC1 48.7%

Figure 7

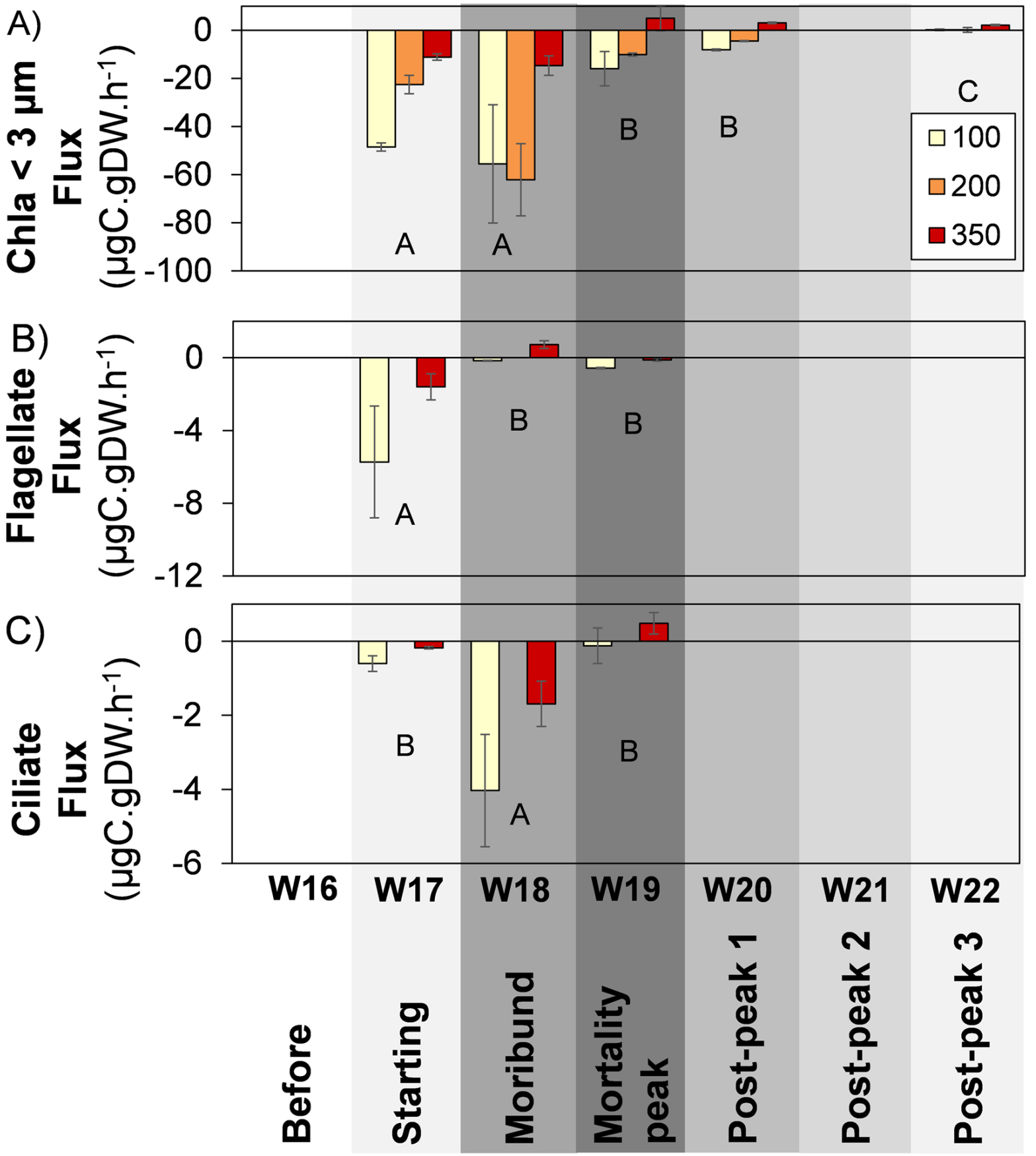
A)
Chla < 3 µm Flux
(µgC.gDW.h-1)
0
-20
-40
-60
-80
-100
A
A
B
B
C
100
200
350
B)
Flagellate Flux
(µgC.gDW.h-1)
0
-4
-8
-12
A
B
B
C)
Ciliate Flux
(µgC.gDW.h-1)
0
-2
-4
-6
B
A
B
W16
W17
W18
W19
W20
W21
W22
Before
Starting
Moribund
Mortality peak
Post-peak 1
Post-peak 2
Post-peak 3

Figure 8

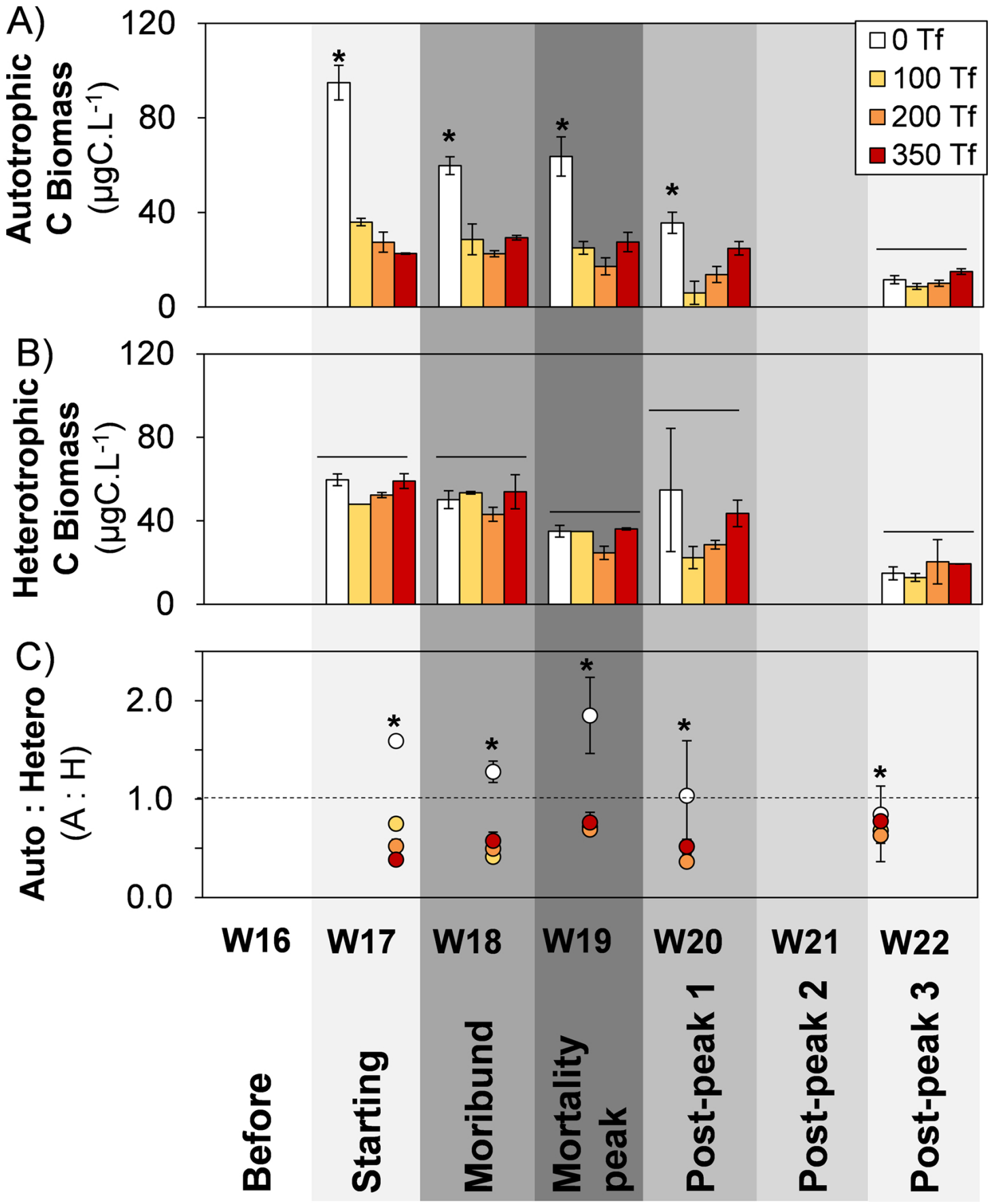
A)
Autotrophic C Biomass (µgC.L-1)
120
80
40
0
0 Tf
100 Tf
200 Tf
350 Tf
B)
Heterotrophic C Biomass (µgC.L-1)
120
80
40
0
C)
Auto : Hetero (A : H)
2.0
1.0
0.0
W16
W17
W18
W19
W20
W21
W22
Before
Starting
Moribund
Mortality peak
Post-peak 1
Post-peak 2
Post-peak 3

Figure 9

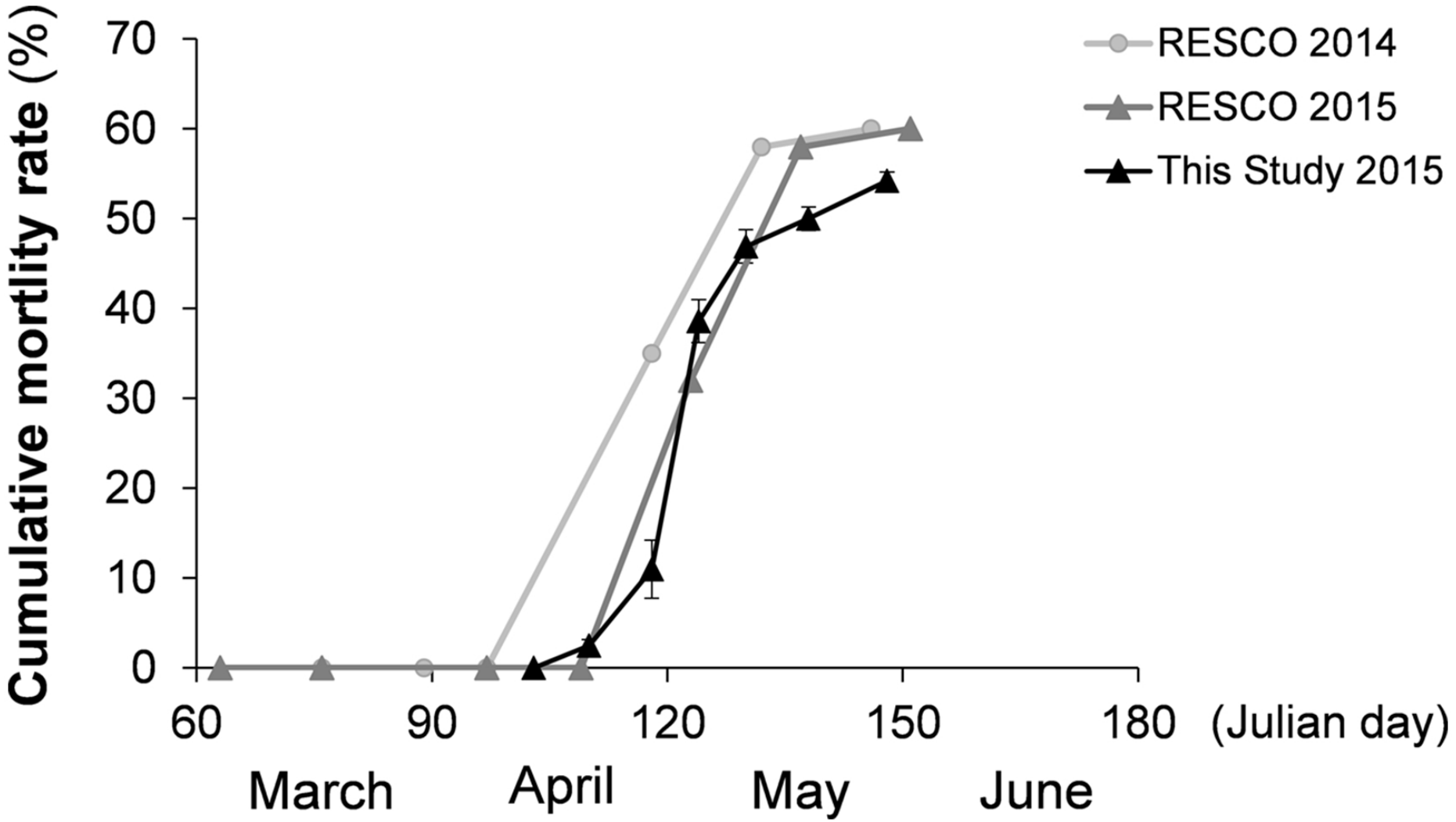
Cumulative mortlity rate (%)
70
60
50
40
30
20
10
0
60
90
120
150
180
(Julian day)
March
April
May
June
RESCO 2014
RESCO 2015
This Study 2015

Figure 10